Production of Diploid Male Gametes in Arabidopsis by Cold-Induced Destabilization of Postmeiotic Radial Microtubule Arrays[1][C][W][OA]

Nico De Storme, Gregory P. Copenhaver, and Danny Geelen*

Department of Plant Production, Faculty of Bioscience Engineering, University of Ghent, 9000 Ghent, Belgium (N.D.S., D.G.); Department of Biology and Carolina Center for Genome Sciences, University of North Carolina, Chapel Hill, North Carolina 27599 (G.P.C.); and Lineberger Comprehensive Cancer Center, University of North Carolina School of Medicine, Chapel Hill, North Carolina 27599 (G.P.C.)

Whole-genome duplication through the formation of diploid gametes is a major route for polyploidization, speciation, and diversification in plants. The prevalence of polyploids in adverse climates led us to hypothesize that abiotic stress conditions can induce or stimulate diploid gamete production. In this study, we show that short periods of cold stress induce the production of diploid and polyploid pollen in Arabidopsis (*Arabidopsis thaliana*). Using a combination of cytological and genetic analyses, we demonstrate that cold stress alters the formation of radial microtubule arrays at telophase II and consequently leads to defects in postmeiotic cytokinesis and cell wall formation. As a result, cold-stressed male meiosis generates triads, dyads, and monads that contain binuclear and polynuclear microspores. Fusion of nuclei in binuclear and polynuclear microspores occurs spontaneously before pollen mitosis I and eventually leads to the formation of diploid and polyploid pollen grains. Using segregation analyses, we also found that the majority of cold-induced dyads and triads are genetically equivalent to a second division restitution and produce diploid gametes that are highly homozygous. In a broader perspective, these findings offer insights into the fundamental mechanisms that regulate male gametogenesis in plants and demonstrate that their sensitivity to environmental stress has evolutionary significance and agronomic relevance in terms of polyploidization.

The spontaneous formation of polyploid species through whole-genome duplication is a major force driving diversification and speciation in plant evolution (Wang et al., 2004). The redundant genomic material produced by polyploidization provides genotypic plasticity that facilitates adaptation and confers enhanced competitiveness compared with diploid progenitors (Adams and Wendel, 2005a, 2005b; Leitch and Leitch, 2008). Molecular analyses suggest that the genomes of most angiosperms (more than 90%) retain evidence of one or more ancient genome-wide duplication events (Cui et al., 2006). Moreover, recently, Wood et al. (2009) established that up to 15% of angiosperm and 31% of gymnosperm speciation events were accompanied by polyploidization. Polyploidization in plants is also commercially beneficial. Many important crop species including wheat (*Triticum aestivum*), potato (*Solanum tuberosum*), tobacco (*Nicotiana tabacum*), coffee (*Coffea arabica*), and numerous fruit varieties are polyploid (Bretagnolle and Thompson, 1995). Although several mechanisms can yield polyploids, it is thought that most polyploid plants are formed by the spontaneous production and fusion of diploid (2n) gametes (Bretagnolle and Thompson, 1995; Ramsey and Schemske, 1998). However, despite the evolutionary and agricultural significance of sexual polyploidization in plants (Ramanna and Jacobsen, 2003), the molecular mechanism underlying 2n gamete formation in natural populations is poorly understood.

Several cytological defects lead to diploid gamete formation in both male and female reproductive lineages. In some species, premeiotic and postmeiotic genome doubling events are reported, but diploid gametes typically result from a defect in one of the two meiotic divisions, a phenomenon referred to as "restitution" (Bretagnolle and Thompson, 1995; Ramsey and Schemske, 1998). Meiotic restitution mechanisms are categorized into three classes: (1) omission of one of the meiotic cell divisions; (2) alterations in meiosis I (MI) or meiosis II (MII) spindle morphology; or (3) defects in meiotic cytokinesis (Ramanna and Jacobsen, 2003). Additionally, depending on the genetic makeup of the resulting 2n gametes, meiotic restitution mechanisms can be further subdivided into two

[1] This work was supported by the National Science Foundation (grant no. MCB–1121563 to G.P.C. and Rijk Zwaan), by the Fund for Scientific Research, Flanders (PhD fellowship to N.D.S. and grant no. G. 0067.09N), and by the LiMiD-Hercules Foundation project (AUGE/013).

* Corresponding author; e-mail danny.geelen@ugent.be.

The author responsible for distribution of materials integral to the findings presented in this article in accordance with the policy described in the Instructions for Authors (www.plantphysiol.org) is: Danny Geelen (danny.geelen@ugent.be).

[C] Some figures in this article are displayed in color online but in black and white in the print edition.

[W] The online version of this article contains Web-only data.

[OA] Open Access articles can be viewed online without a subscription.

www.plantphysiol.org/cgi/doi/10.1104/pp.112.208611

classes: first division restitution (FDR) and second division restitution (SDR). In FDR, the sister chromatids disjoin and segregate to opposite poles, yielding 2n gametes that largely retain the heterozygosity of the parental plant. In SDR, sister chromatids do not disjoin in MII and segregate to the same pole, generating highly homozygous 2n gametes (Köhler et al., 2010).

Several genes governing 2n gamete formation have been identified and characterized in potato, maize (*Zea mays*), and Arabidopsis (*Arabidopsis thaliana*; Consiglio et al., 2004; Brownfield and Köhler, 2011). Mutations in Arabidopsis *DYAD/SWITCH1* and maize *ARGONAUTE104* (*AGO104*) and *AM1* induce a complete loss of MI and, consequently, convert the meiotic cell cycle into a mitotic one (Ravi et al., 2008; Pawlowski et al., 2009; Singh et al., 2011). Lesions in Arabidopsis OSD1/GIG1 and TAM/CYCA2;1, two proteins involved in progression of the meiotic cell cycle, cause a complete loss of MII, generating highly homozygous 2n gametes in both male and female meiosis (d'Erfurth et al., 2009, 2010). Spindle-based meiotic restitution mechanisms have been reported in both Arabidopsis *jason* and *atps1* mutants and in the potato *ps* mutant, in which parallel, fused, and tripolar spindles in male MII lead to the formation of FDR 2n spores (Mok and Peloquin, 1975; d'Erfurth et al., 2008; De Storme and Geelen, 2011). Disruption of postmeiotic male cytokinesis, which is regulated by a mitogen-activated protein kinase (MAPK) kinase signaling pathway, also results in polyploid gametes. Mutations in *TES/STUD/AtNACK2*, *MKK6/ANQ1*, and *MPK4*, three main components of the cytokinetic MAPK signaling cascade, induce a complete loss of cytokinesis following male meiosis, generating fully restituted tetraploid pollen grains (Hulskamp et al., 1997; Spielman et al., 1997; Soyano et al., 2003; Zeng et al., 2011).

Despite progress on understanding cytological mechanisms and genetic factors governing the formation of 2n gametes in natural populations, less is known about the environmental factors involved. There is evidence that 2n gamete production can be stimulated by both biotic and abiotic stresses, such as nutritional deprivation, wounding, disease, herbivory, and temperature stress (Ramsey and Schemske, 1998). In *Lotus tenuis*, temperature stresses, and in particular high temperatures, increase the level of parallel spindle-driven 2n gamete production (Negri and Lemmi, 1998). Similarly, in rose (*Rosa* spp.), short periods of high temperature (48 h at 30°C–36°C) can induce cytomixis and parallel and tripolar spindles at male metaphase II, generating dyads and triads at the end of male sporogenesis (Pécrix et al., 2011). Low-temperature environments can also stimulate 2n gamete formation. For example, *Solanum phureja* grown in cool field environments produces more restituted spores compared with lines grown under normal conditions (McHale, 1983). Similarly, in *Datura* spp. and *Achillea borealis*, unreduced pollen formation is higher at low temperatures (Ramsey and Schemske, 1998; Ramsey, 2007). Recently, Mason et al. (2011) demonstrated that cold stress significantly stimulates 2n pollen production in some interspecific *Brassica* spp. hybrids. Temperature-induced diploid gamete formation is not restricted to plants. Low temperatures have also been shown to stimulate the formation of 2n spores in some animal species, particularly among fish and amphibians (Bogart et al., 1989; Mable et al., 2011). Moreover, ecological population studies have demonstrated that polyploid plant and animal species occur more frequently at higher altitudes and at latitudes closer to the poles (Beaton and Hebert, 1988; Barata et al., 1996; Dufresne and Hebert, 1998), leading to the suggestion that cold climates stimulate the production of polyploid gametes.

In this study, we demonstrate that short periods of cold stress induce a development-specific production of meiotically restituted spores in Arabidopsis, which thereby constitutes an ideal model system to identify potential cytological and molecular factors involved in stress-induced sexual polyploidization. Using a combination of cytological and genetic approaches, we reveal the cytological basis for cold-induced meiotic restitution and additionally demonstrate that restituted binuclear and polynuclear spores spontaneously develop into diploid and polyploid pollen grains. We also use pollen tetrad-based segregation analysis to monitor the genetic makeup of cold-induced 2n gametes and Arabidopsis mutants to examine the potential role of some candidate regulators (e.g. TAM/CYCA1;2 and MKK2) in the sensitivity of male meiosis to low-temperature stress.

RESULTS

Cold Stress Induces Diploid and Polyploid Pollen Grains in Arabidopsis

To determine whether the ploidy of Arabidopsis male gametes is sensitive to low-temperature stress, flowering plants were put in a climate chamber at 4°C to 5°C for 20 or 40 h to mimic approximately 1 and 2 d of cold stress, respectively. After transfer back to normal growing conditions, the frequency of higher ploidy gamete formation was quantified by assessing pollen diameter (De Storme and Geelen, 2011). Although no large pollen were observed during the first 5 d following cold stress, enlarged pollen were detected at 6, 7, and 8 d after treatment (Fig. 1A). In both temperature regimes, the production of larger pollen grains showed a maximum at 7 d post treatment (dpt) and displayed lower frequencies the day before and after. The frequency of flowers producing larger pollen upon 20 or 40 h of cold shock was 6.3%, 34.8%, and 13.5% or 11.5%, 28.4%, and 0.0% at 6, 7, and 8 dpt, respectively (Supplemental Table S1). Although Arabidopsis inflorescences typically have two to four open flowers per day, no more than one appeared to produce larger pollen, indicating that the cold treatment acts at a specific time point in the plant's reproductive development. Moreover, at 7 dpt, all inflorescences had at least one flower that contained larger pollen, a consistency that is reflected by the similar frequency of flowers producing enlarged spores

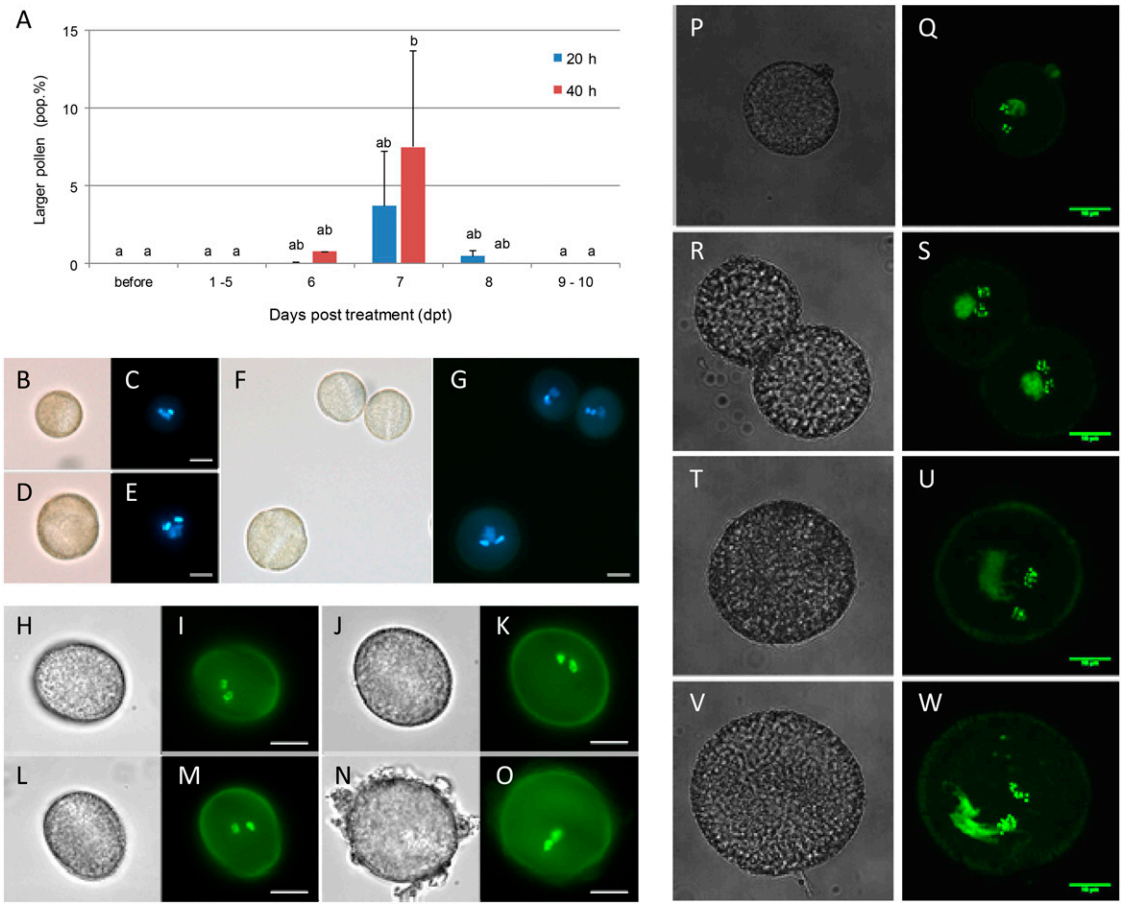

Figure 1. Cold stress induces the formation of diploid and polyploid pollen. A, Histogram showing the frequency of larger pollen grains produced 1 to 10 d following cold treatment of young flowering Arabidopsis plants (20 and 40 h, 4°C–5°C). B to G, DAPI staining of wild-type (B and C) and cold-treated (D–G) pollen 7 dpt (40 h, 4°C–5°C). H to O, Mature pollen of the *pMGH3*::*H2B-GFP* marker line under normal conditions (H and I) and 7 d post cold treatment (40 h, 4°C–5°C; J–O). P to W, Mature pollen of the gamete-specific *pWOX2*::*CENH3-GFP* centromeric labeling line under control conditions (P and Q) and 7 d post cold treatment (40 h, 4°C–5°C; R–W) imaged by confocal Z-stacking. Fluorescent images are Z-axis projections. Three-dimensional centromere counting in sperm of cold-induced enlarged spores reveals either 10 (S), 15 (U), or 20 (W) chromosomes. Bars = 10 μm.

in both treatments (34.8% and 28.4% in 20- and 40-h treatments, respectively). Furthermore, since the 40-h treatment produced more enlarged pollen at 7 dpt (26.4% on a per flower basis, 9.3% on a population basis) compared with the 20-h cold treatment (10.7% and 3.7%, respectively), the duration of cold treatment appeared positively correlated with the frequency of large pollen production (Supplemental Table S1). These data suggest that the cold-induced mechanism of enlarged pollen production operates at a specific developmental stage in male gametogenesis occurring 7 to 8 d before the mature pollen stage.

To estimate the ploidy level and number of nuclei in the cold-induced large pollen, we monitored male gametophytic nuclei using 4′,6-diamidino-2-phenylindole (DAPI) staining of mature pollen grains. Although the nuclear configuration in all large pollen appeared normal, with one less-condensed vegetative nucleus and two highly condensed sperm nuclei (Fig. 1, B–G), both types of gametophytic nuclei appeared significantly bigger compared with haploid controls, indicating that the enlarged pollen were diploid and/or polyploid (Coleman and Goff, 1985; Li et al., 2009; De Storme and Geelen, 2011). Similar observations were made in cold-treated plants carrying a *pMGH3*::*H2B-GFP* reporter construct. This transgene specifically labels histone H2B in the nucleosomes of all male gametophytic nuclei, from the early microspore to the mature pollen stage (Brownfield et al., 2009), and enables the in vivo estimation of the gametophytic nuclear DNA content. Upon cold stress (7 dpt), enlarged *pMGH3*::*H2B-GFP* pollen grains (n = 54) all contained two enlarged sperm nuclei with increased fluorescence intensity, indicative of increased DNA content (Fig. 1, H–O). In order to determine the exact ploidy level of the enlarged sperm nuclei, we quantified the number of chromosomes by using plants harboring a *pWOX2*::*CENH3-GFP* reporter construct. This reporter labels the centromere-specific histone H3-like protein

HTR12 (Talbert et al., 2002) in all stages of microspore development and thus enables the quantification of gametophytic chromosome numbers from the early microspore to the mature pollen stage (De Storme and Geelen, 2011). Under control conditions, sperm nuclei of *pWOX2*::*CENH3-GFP* pollen grains consistently displayed five centromeric dots (Fig. 1, P and Q; $n = 135$), reflecting the basic set of five chromosomes present in a haploid nucleus. In contrast, in the cold-induced enlarged spores (7 dpt), a higher number of centromeres was observed (Fig. 1, R–W), indicating an increased gametophytic chromosome number. Moreover, as enlarged pollen always contained 10, 15, or 20 centromeric dots in its sperm nuclei ($n = 38$), we conclude that cold stress does not generate gametophytic aneuploidy but instead induces the formation of diploid, triploid, and tetraploid male spores.

Cold-Induced Diploid and Polyploid Spores Originate from Aberrations in Meiotic Cell Division

Diploid and polyploid gametes can be formed by somatic genome doubling or by meiotic restitution mechanisms (Bretagnolle and Thompson, 1995). To differentiate between these possibilities, we monitored male meiosis in cold-shocked *qrt1-2*$^{-/-}$ plants. Due to the loss of QRT1 activity, a pectin methylesterase involved in postmeiotic spore release, the four products of *qrt1-2*$^{-/-}$ male sporogenesis remain attached and pollen grains are released as tetrads (Francis et al., 2006). This allows for the nondestructive visual analysis of the outcome of male meiosis (Johnson-Brousseau and McCormick, 2004). In line with this, we found that untreated *qrt1-2*$^{-/-}$ control plants always shed pollen tetrads with four haploid spores ($n = 250$; Fig. 2A). Cold-treated *qrt1-2*$^{-/-}$ plants (7 dpt), on the other hand, produced enlarged pollen grains in meiotically restituted nontetrad configurations, including dyads (balanced and unbalanced), triads, and, in some rare cases, monads, indicating that the cold-induced formation of diploid and polyploid pollen results from a restitution of the meiotic cell division (Fig. 2, B–E). Although balanced dyads and especially triads are typically observed in restitutional mechanisms conferred by defects in MII spindle orientation (e.g. Arabidopsis *atps1* and *jason* mutants; d'Erfurth et al., 2008; De Storme and Geelen, 2011), the additional presence of monads points toward a defect in prophase I or in postmeiotic cell wall formation (Spielman et al., 1997; d'Erfurth et al., 2010).

In order to estimate the developmental time frame at which cold stress induces a restitution of the meiotic cell cycle, we next assessed the meiotic tetrad configuration of cold-stressed *qrt1-2*$^{-/-}$ plants (40 h, 4°C–5°C) at the early uninuclear microspore stage during the first 3 d following cold treatment. During and just after (0–8 h post treatment [hpt]) cold treatment, *qrt1-2*$^{-/-}$ spores always had a normal tetrad configuration (Fig. 2F; $n > 500$). In contrast, at 30 hpt, we observed restituted figures such as triads (Fig. 2I; 24.3%), balanced and unbalanced dyads (Fig. 2, G and H; 16.0% and 7.1%), and a small subset of monads (Fig. 2, J and P; 1.0%; $n = 775$). Strikingly, in the following days, no restituted figures were observed in the uninuclear *qrt1-2*$^{-/-}$ microspore stage. Similar observations were made in wild-type plants, in which tetrad stages can only be assessed in a short window following meiotic cytokinesis before microspore release (Supplemental Fig. S1A). In cold-treated wild-type plants, meiotically restituted figures, such as dyads, triads, and monads, were only observed 1 dpt (20–24 hpt; Supplemental Fig. S1, B–E). These findings suggest that cold stress-induced diploid and polyploid spores originate from a meiotic restitution event that operates at a specific phase or time frame in the meiotic cell division program, specifically occurring 20 to 24 h before tetrad microspore release.

Binuclear and Polynuclear Microspores Are Formed by Cold-Induced Defects in Postmeiotic Cell Plate Formation

Because meiotic restitution is usually caused by defects in chromosome segregation or nuclear positioning, we assessed the postmeiotic nuclear configuration (number of nuclei and position inside the meiocyte) at the tetrad stage using acetocarmine staining. Similar to tetrad meiocytes under normal conditions (Fig. 2L), cold-shocked dyads, triads, and monads always contained four equally sized, tetrahedrally arranged nuclei (Fig. 2, M–P), suggesting that the progression of the meiotic cell cycle was not affected. However, in contrast to control tetrads, in which all four haploid nuclei are physically isolated from each other through the establishment of internuclear cell walls (tetrad, n+n+n+n), cold-shocked meiotic products occasionally lacked one or more of these internuclear cell walls, and haploid nuclei were configured in syncytial groups of two (triads, 2n+n+n; and balanced dyads, 2n+2n), three (unbalanced dyads, 3n+n), or four (monads, 4n; Fig. 2, M–P). Consequently, upon spore release, binuclear, trinuclear, and tetranuclear microspores were formed (Fig. 2, R–U), instead of the normal uninuclear products (Fig. 2Q). Quantitative analysis at this stage demonstrated that cold stress generates a higher frequency of binuclear microspores (2N, 6.0%) compared with trinuclear and tetranuclear spores (3N, 0.8%; and 4N, 0.1%, respectively; $n = 2{,}457$). These frequencies closely correspond to the meiotic tetrad stage observations (in control and *qrt1-2*$^{-/-}$ backgrounds), displaying the predominant formation of cold-induced balanced dyads (2n+2n) and triads (2n+n+n).

To determine the number of chromosomes in individual nuclei of low-temperature-induced binuclear and polynuclear spores, we used the *pWOX2*::*CENH3-GFP* background to perform centromere-based chromosome counts at the early microspore stage. In the cold-induced binuclear, trinuclear, and tetranuclear microspores ($n = 52$), single nuclei were found to

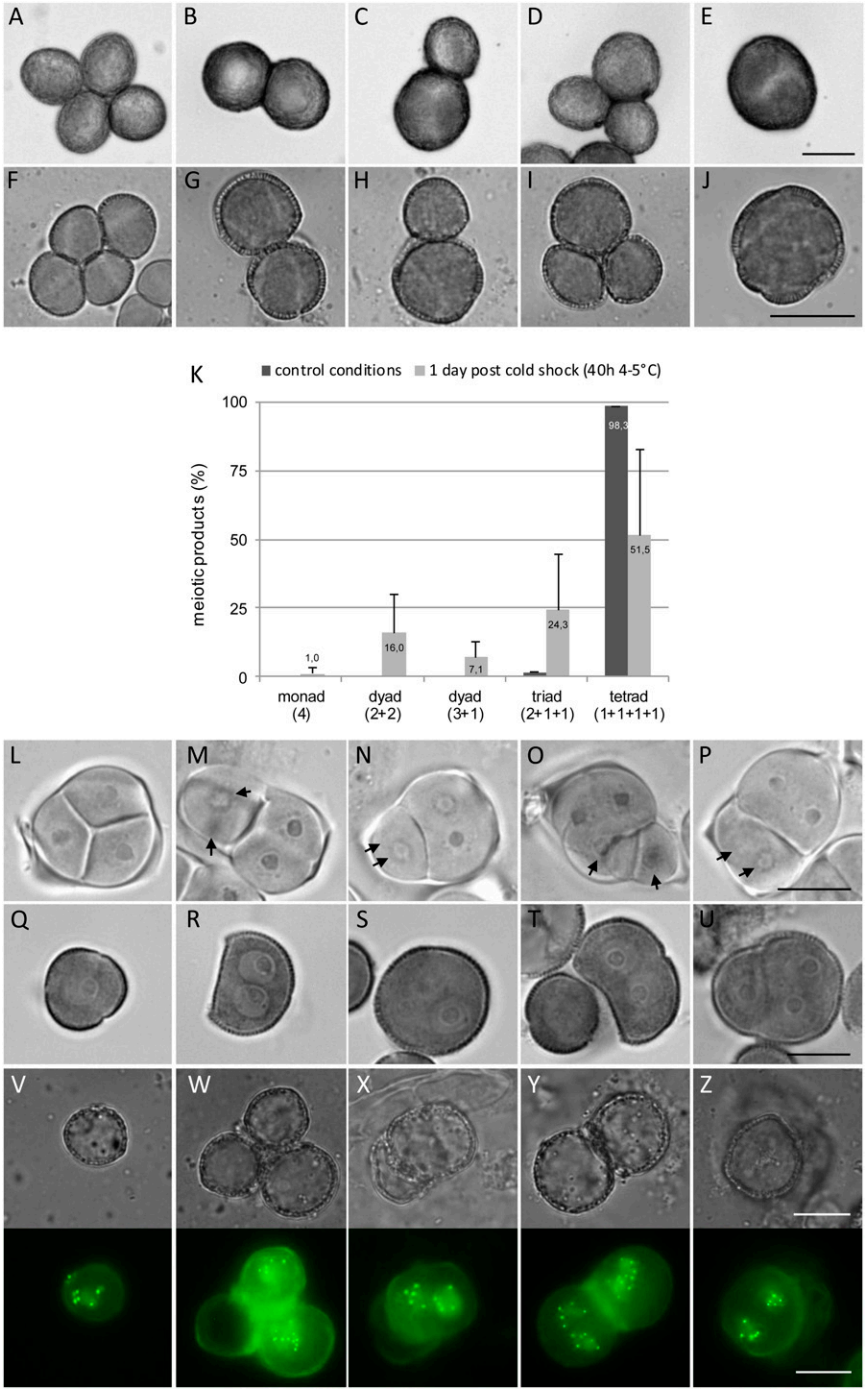

Figure 2. Cold-induced defects in male meiotic cell plate formation lead to binuclear and polynuclear spores. A to E, Arabidopsis *qrt1-2*$^{-/-}$ sheds mature pollen in a tetrad configuration under normal conditions (A) but shows altered configurations 7 dpt (40 h, 4°C–5°C), including balanced dyads (B), unbalanced dyads (C), triads (D), and monads (E). Bar = 20 μm. F to J, Cytological analysis of the early microspore stage in *qrt1-2*$^{-/-}$ shows normal tetrads (F) 0 d post treatment (40 h, 4°C–5°C) but reveals the presence of balanced dyads (G), unbalanced dyads (H), triads (I), and monads (J) 1 d later (1 dpt). Bar = 10 μm. K, Graphical representation of the frequency of cold-induced meiotic restitution configurations in the *qrt1-2*$^{-/-}$ background 1 d post cold treatment (40 h, 4°C–5°C; n = 500 for control conditions and n = 775 for cold treatment). L to P, Acetocarmine staining of the meiotic outcome of wild-type male sporogenesis under normal conditions (L) and 1 d post cold shock (40 h, 4°C–5°C; M–P). Due to the tetrahedral positioning, one or two nuclei always appear out of focus (indicated by arrows). Q to U, Orcein staining of early microspores of untreated (Q) and cold-stressed (R–U) wild-type plants 30 h post treatment (40 h, 4°C–5°C). V to Z, Bright-field and fluorescence images of *pWOX2*::*CENH3-GFP*-mediated in vivo centromere labeling of gametophytic nuclei in untreated (V) and cold-stressed (W–Z) microspores 30 hpt. Fluorescent images were obtained by maximum intensity projections of original Z-stacks. The increased number (more than five) of centromeric dots observed in some spores (W and Y) is caused by the overlay of two single haploid nuclei. Note the Qrt1^{-}-like appearance of binuclear spores in an ectopic dyad or triad configuration (V and X). Bars = 10 μm. [See online article for color version of this figure.]

contain five centromeric dots (Fig. 2, W–Z), similar to the nuclei of wild-type haploid uninuclear spores (Fig. 2V). As these observations suggest proper meiotic chromosome segregation, we conclude that cold stress does not affect the reductional division of chromosomes but instead interferes with the formation and/or maintenance of the internuclear cell plates at the end of MII.

To define the specific meiotic stage at which cold stress induces alterations in the cell division process, we performed shorter cold shock treatments (1, 2, or 4 h at 4°C–5°C) and assayed binuclear or polynuclear spore formation 0, 1, and 2 dpt. Strikingly, in this experiment, we found that even the shortest treatment of 1 h induced the formation of meiotically restituted binuclear and/or trinuclear spores at 1 dpt. At other time points (e.g. immediately after the treatment or 2 dpt), only uninuclear spores were observed (Supplemental Fig. S2). Similarly, the 2- and 4-h treatments also resulted in the formation of binuclear and

polynuclear spores 1 dpt. However, in contrast to the 1-h treatment, which only generated 2.4% of binuclear spores, the 2- and 4-h treatment yielded 7.0% and 7.6% binuclear spores, respectively, together with the occasional formation of trinuclear spores (Supplemental Fig. S2A). Moreover, as the 40-h cold treatment was found to yield an average frequency of 17% binuclear and additional trinuclear and tetranuclear spores, the duration of cold stress was found to be positively correlated with the severity of the meiotic restitution phenotype. These observations support the hypothesis that cold-induced cytological alterations cause male meiotic restitution at a specific stage in the meiotic cell division program occurring 22 to 26 h prior to the resolution of the meiotic tetrad (e.g. telophase II, postmeiotic cytokinesis).

Polynuclear Microspores Fuse before the First Gametophytic Division

To monitor how cold stress-induced binuclear and polynuclear microspores develop into diploid, triploid, and tetraploid pollen grains, we assessed the nuclear dynamics of both binuclear and polynuclear gametes during microspore development. In cold-shocked young microspores (1 dpt), both acetocarmine staining and the *pMGH3*::*H2B-GFP* reporter assay showed the presence of two to four equally sized nuclei in the larger, often bean-shaped microspores (Fig. 3, B, C, H, and I), instead of the single nucleus observed in control spores (Fig. 3, A and G). One day later, however, enlarged microspores generally showed one large nucleus instead of the two smaller ones, indicating that the coallocated haploid nuclei fused during microspore development. As a result, at the binuclear microspore stage following pollen mitosis I, the enlarged spores (n = 82) did not show a polynuclear phenotype but instead contained the normal set of two heteromorphic nuclei (one vegetative and one generative), which were substantially larger than the corresponding haploid nuclei (Fig. 3, D–F and J–L). These observations indicate that, although cold stress-induced microspores contain more than one haploid nucleus, the spontaneous fusion of nuclei at the late microspore stage enables a normal progression of the subsequent male gametophytic development process and leads to the formation of polyploid male gametes with two sperm nuclei and one vegetative nucleus.

We also noted that cold-stressed microspores (1–3 dpt) and mature pollen grains (6–8 dpt) often remained physically attached to each other, typically displaying a meiotically restituted (e.g. dyad, triad) or tetrad configuration. Indeed, despite being *QRT1*$^{+/+}$, cold-stressed wild-type, *pWOX2*::*CENH3-GFP* (Figs. 1, R and S, and 2, W and Y), and *pMGH3*::*H2B-GFP* (Fig. 3, C and F) microspores often appeared in a *qrt1*$^{-/-}$-like dyad, triad, or tetrad configuration (approximately 20%),

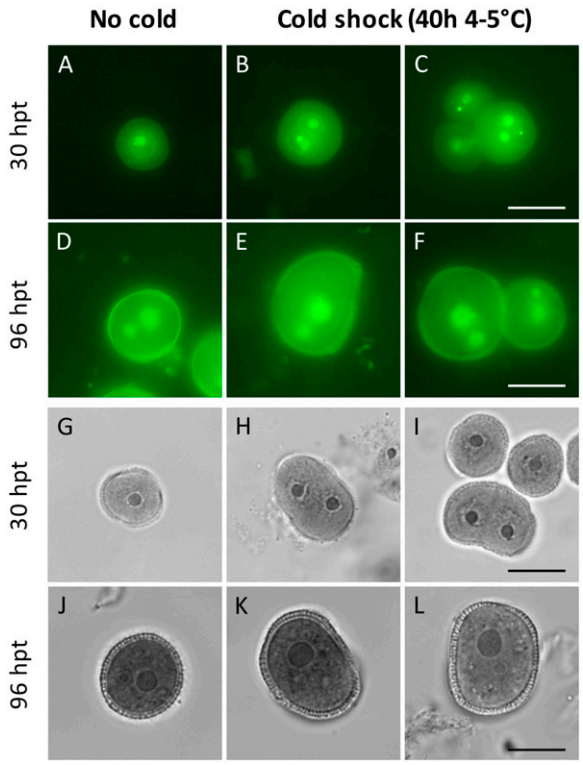

Figure 3. Nuclei of cold-induced binuclear and polynuclear spores fuse before the bicellular microspore stage. A to C, Unicellular-stage microspores containing the *pMGH3*::*H2B-GFP* male gametophyte-specific histone-labeling construct under normal conditions (A) and 30 h post cold treatment (40 h, 4°C–5°C; B and C). D to F, Bicellular-stage *pMGH3*::*H2B-GFP* spores under control conditions (D) and 96 h post cold shock (E and F). G to L, Acetocarmine staining of microspores at the unicellular (G–I) and bicellular (J–L) stages isolated from untreated (G and J) and cold-stressed (30 hpt [H and I] and 96 hpt [K and L]) wild-type plants. Bars = 10 μm. [See online article for color version of this figure.]

indicating that cold stress not only affects meiotic cell wall formation but additionally interferes with the proper release of microspores at the end of male sporogenesis.

Cold-Induced Meiotic Restitution Produces Primarily SDR-Type 2n Gametes

Since cold-induced binuclear spores lead to the formation of diploid pollen grains, we questioned whether restituted 2n pollen are genotypically equivalent to FDR or SDR. Cold-induced diploid gametes were genotyped using the Fluorescent Tagged Line (FTL) system (Francis et al., 2007). In this system, transgenic markers expressing fluorescent proteins under the control of the postmeiotic, pollen-specific *LAT52* promoter are used in a *qrt1-2*$^{-/-}$ mutant background (Twell et al., 1990; Preuss et al., 1994). Plants that are hemizygous for an FTL marker (m/−) shed pollen tetrads that reveal meiotic segregation by expressing the fluorescent protein in a 2:2 fluorescent:

nonfluorescent pattern (m/m/−/−; Berchowitz and Copenhaver, 2008).

In meiotically restituted dyads and triads, sister chromatids either disjoin or not, leading to the formation of highly heterozygous (FDR) or homozygous (SDR) 2n gametes, respectively. Thus, by monitoring the segregation of a heterozygous FTL marker in *qrt1-2*$^{-/-}$ dyads and triads, both FDR- and SDR-type 2n gametes can be discriminated. It should be noted, however, that meiotic recombination between the marker and the centromere can transfer the reporter construct between homologous chromosomes and consequently interfere with the segregation analysis. To minimize the effects of recombination, two FTL lines with markers close to the centromere (FTL 3253 and I4a, containing two closely linked markers, FTL 1323 and FTL 424) and one line with a more distally located marker (FTL 1273) were used in this study (Fig. 4G).

For the markers close to the centromere (i.e. FTL 3253 and I4a), cold stress-induced dyads generally showed one fluorescent and one nonfluorescent spore (mm/–; 67.8% and 81.0%, respectively; Fig. 4B; Table I). In these dyads, one of the 2n pollen grains contained the two sister chromatids carrying the reporter construct (mm), whereas the other one inherited the other two nontransgenic sister chromatids (–). This segregation pattern demonstrates that cold-shocked dyads generally contain highly homozygous 2n spores and thus provides evidence that cold stress induces a cytological meiotic restitution mechanism equivalent to SDR. However, the presence of dyads with two fluorescent pollen grains (m–/m–; 19.0%, 32.2%, and 51.2% for markers I4a, FTL 3253, and FTL 1273) suggests that cold stress also generates a fraction of 2n dyads through an FDR-type restitution (Fig. 4C; Table I).

Similarly, in cold stress-induced triads, a relatively high number of homozygous SDR-type 2n gametes (Fig. 4, D [mm/−/−] and E [–/m/m]) was observed for the centromeric marker FTL 3253 (63.3%) compared with the relatively low level of heterozygous FDR-type diploid gametes (m–/m/–; 36.7%; Fig. 4F; Table I). As some of these FDR-type spores can result from restitution of the second division (through a recombination between marker and centromere), it is difficult to ascertain the true number of spores that result from an FDR-like mechanism. Thus, based on the FTL segregation analysis, we conclude that cold-induced defects in (post) meiotic cytokinesis primarily lead to the formation of SDR-type 2n male gametes but may also induce some FDR-type 2n spores.

To verify that the subpopulation of full fluorescent dyads (m–/m–) in both the Ia4 and FTL 3253 heterozygous backgrounds really reflects the occurrence of 2n gametes generated by FDR-type restitution, we analyzed the cold-stress meiotic response in the *atspo11-1-3*$^{-/-}$ mutant background. Due to a complete loss of double-strand break formation, *atspo11-1-3*$^{-/-}$ prophase I meiocytes produce univalents instead of bivalents, which segregate randomly to form unbalanced tetrads and polyads (Grelon et al., 2001).

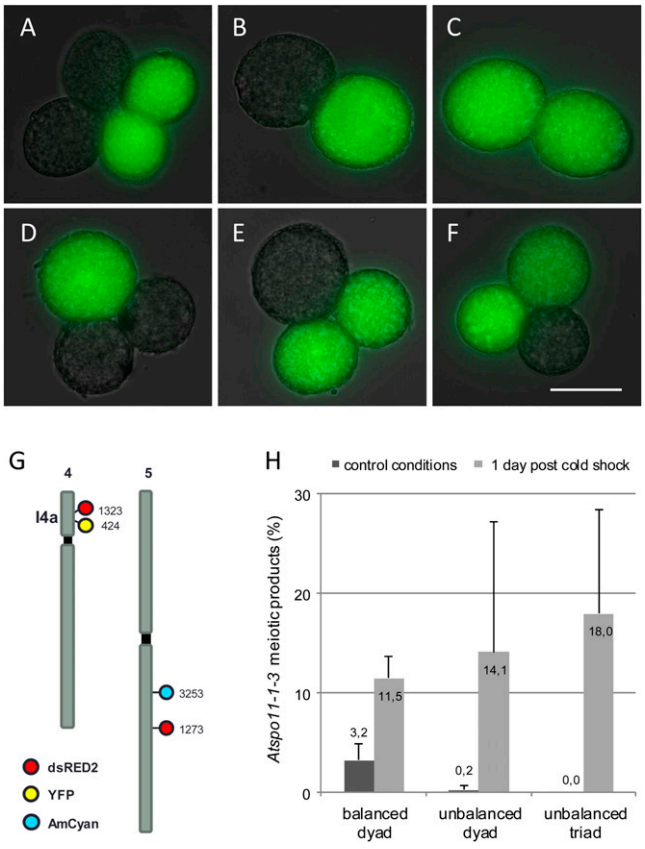

Figure 4. Cold stress primarily produces SDR-type 2n gametes. A to F, Genotypic characterization of cold-induced 2n gametes using the *qrt1-2*$^{-/-}$ FTL marker assay (FTL 424, yellow fluorescent protein [YFP]). Segregation of a heterozygous FTL construct in *qrt1-2*$^{-/-}$ pollen tetrads always shows a 2:2 fluorescent:nonfluorescent ratio (A; m/m/−/−). In meiotically restituted dyads, the presence of one fluorescent spore suggests an SDR mechanism (B; mm/–), whereas two fluorescent spores point toward an FDR-type meiotic restitution (C; m−/m−). Similarly, triads in which the enlarged diploid spore is fluorescent whereas the two haploid ones are not (D; mm/−/−), and vice versa (E; −/m/m), indicate an SDR-type restitution. Triads in which both the diploid spore and one haploid spore are fluorescent (F; m−/m/−) are indicative for FDR. Bar = 20 μm. G, Genomic positions of FTL markers used in this study. H, Histogram showing the frequency of balanced dyads, unbalanced dyads, and triads in *atspo11-1-3*$^{-/-}$ Arabidopsis male meiosis under control conditions and 1 d after cold treatment (40 h, 4°C–5°C). Mean frequency numbers are listed in the plot bars. Frequencies of other meiotic products, such as tetrads, polyads, and monads, are not represented here (Supplemental Table S2). [See online article for color version of this figure.]

Because FDR meiotic restitution mechanisms (e.g. parallel spindles, loss of first meiotic cell plate formation) typically regroup the unbalanced MI chromosome sets into euploid numbers at MII, *atspo11-1-3*$^{-/-}$ can be used as a bioassay to detect the presence of FDR meiotic restitution mechanisms (d'Erfurth et al., 2008; De Storme and Geelen, 2011). SDR restitution mechanisms (e.g. loss of MII or loss of second cell plate formation), on the other hand, do not regroup unbalanced *atspo11-1-3*$^{-/-}$ chromosome sets in MII

Table I. *FTL-based genotypic characterization of cold-induced 2n pollen*

Genotyping 2n gametes was performed in cold-induced dyads and triads using heterozygous FTL markers in the *qrt1-2*$^{-/-}$ mutant background. mm/–, mm/–/–, and –/m/m fluorescent configurations constitute marker-specific homozygosity (SDR) for the diploid spore, whereas m–/m– and m–/m/– arrangements point towards heterozygosity for that specific marker.

qrt1-2$^{-/-}$ FTL Marker $^{(m/-)}$				Dyads			Triads			
Name	Label	Chromosome	Position	*n*	m−/m−	mm/–	*n*	mm/−/−	m−/m/−	–/m/m
					%					
FTL 424 (I4a)	Y/−	4	Centromeric	21	19.0	81.0	–	–	–	–
FTL 1323 (I4a)	R/−	4	Centromeric	21	19.0	81.0	–	–	–	–
FTL 3253	C/−	5	Centromeric	121	32.2	67.8	267	33.0	36.7	30.3
FTL 1273	R/−	5	Midchromosomal	121	51.2	48.8	267	22.1	52.1	25.8

and consequently generate unbalanced dyads. Under normal growth conditions, *atspo11-1-3*$^{-/-}$ male sporogenesis produces unbalanced tetrads and polyads, a small proportion of dyads (3.2% balanced and 0.2% unbalanced), and no triads (Fig. 4H; Supplemental Table S2). One day after cold stress, however, a strong increase in dyads (25.6%; balanced + unbalanced) and triads (18.0%) was observed (Fig. 4H; Supplemental Table S2). Moreover, although cold stress in *atspo11-1-3*$^{-/-}$ generally induces the formation of unbalanced dyads (14.1%; $P = 0.141$), confirming the prevalent induction of SDR-type meiotic restitution, a significant increase in balanced dyad formation was also observed (11.5%; $P = 0.007$; Fig. 4H; Supplemental Table S2). This finding supports the earlier suggestion that the cytological mechanism underlying cold-induced meiotic restitution not only generates 2n spores through an SDR-type restitution but also produces a subset of 2n spores through an FDR-type restitution. This combinatorial formation of a majority of SDR-type and a subset of FDR-type 2n gametes is in agreement with the earlier observed cold-induced defects in postmeiotic cell plate formation and additionally indicates that defects in cell plate formation predominantly occur between chromosome sets that disjoined in MII.

Cold-Stressed Male Meiocytes Display Regular Reductional Chromosome Segregation

Aberrations in (post)meiotic cell plate formation and the associated formation of diploid and polyploid male spores may originate from alterations in the meiotic cell cycle program. For example, loss of TAM/CYCA1;2, a cyclin that regulates meiotic cell cycle progression, induces a complete loss of MII and produces meiotic dyads with SDR 2n spores (d'Erfurth et al., 2010; Wang et al., 2010). However, in contrast to most *tam* mutants, which display a complete loss of MII, the "weak" temperature-sensitive mutant *tam-1* only shows a delay in meiotic cell cycle progression and typically generates cell plate-defective dyads (4N2C; four nuclei in two cells) and triads (4N3C) at the end of MII (Magnard et al., 2001; Wang et al., 2004).

As similar restituted products are observed in cold-treated wild-type meiocytes, we hypothesized that cold-induced defects in male meiosis could be caused by altered TAM function. We tested this hypothesis by cold treating loss-of-function *tam-2* and by analyzing the male meiotic outcome 1 dpt. In nonstressed *tam-2* plants, male sporogenesis predominantly generates balanced dyads (Fig. 5A; 82.9%) together with a minor subset of triads and tetrads (13.3% and 3.8%, respectively), but no monads. Upon cold treatment (40 h at 4°C–5°C, 1 dpt), however, *tam-2* not only produced dyads (95.0%) and triads (0.3%) but also generated a subset of monads (Fig. 5, B, D, and E; 4.7%). In the monads, the two diploid nuclei generated by restitution of MII were not separated by a callosic cell wall but instead remained together to form a binuclear meiotic product (Fig. 5, D and E, black arrows). Consistent with this, we observed a subset of significantly larger pollen grains (presumably 4n) in the *tam-2* diploid pollen population at the end of male spore development at 7 dpt (Fig. 5, C and F).

This experiment demonstrates that cold stress has an additive effect (loss of cell plate formation) on the *tam-2* meiotic phenotype, indicating that cold-induced defects in postmeiotic cell plate formation do not depend on CYCA1;2 and are not directed by OSD1, the other major protein involved in meiotic cell cycle progression. Indeed, although double *tam/osd1* plants also generate monads at the end of male meiosis (loss of MI and MII), these cells only contain one fully restituted tetraploid nucleus (d'Erfurth et al., 2010), whereas cold stress-induced *tam-2* monads consistently contain two diploid nuclei (Fig. 5, D and E; $n = 16$). Additionally, our data suggest that low-temperature shocks specifically affect postmeiotic cytokinesis and/or cell wall formation without interfering with meiotic chromosome segregation.

To investigate the effect of cold stress on meiotic chromosome segregation, we next examined DAPI-stained chromosome spreads of 4- and 40-h cold-stressed male meiocytes. Except for the final tetrad stage, all meiotic stages under cold stress conditions had similar chromosomal behavior and nuclear configuration compared with control conditions (Fig. 5, G–U). In both 4- and 40-h cold-treated meiocytes, the

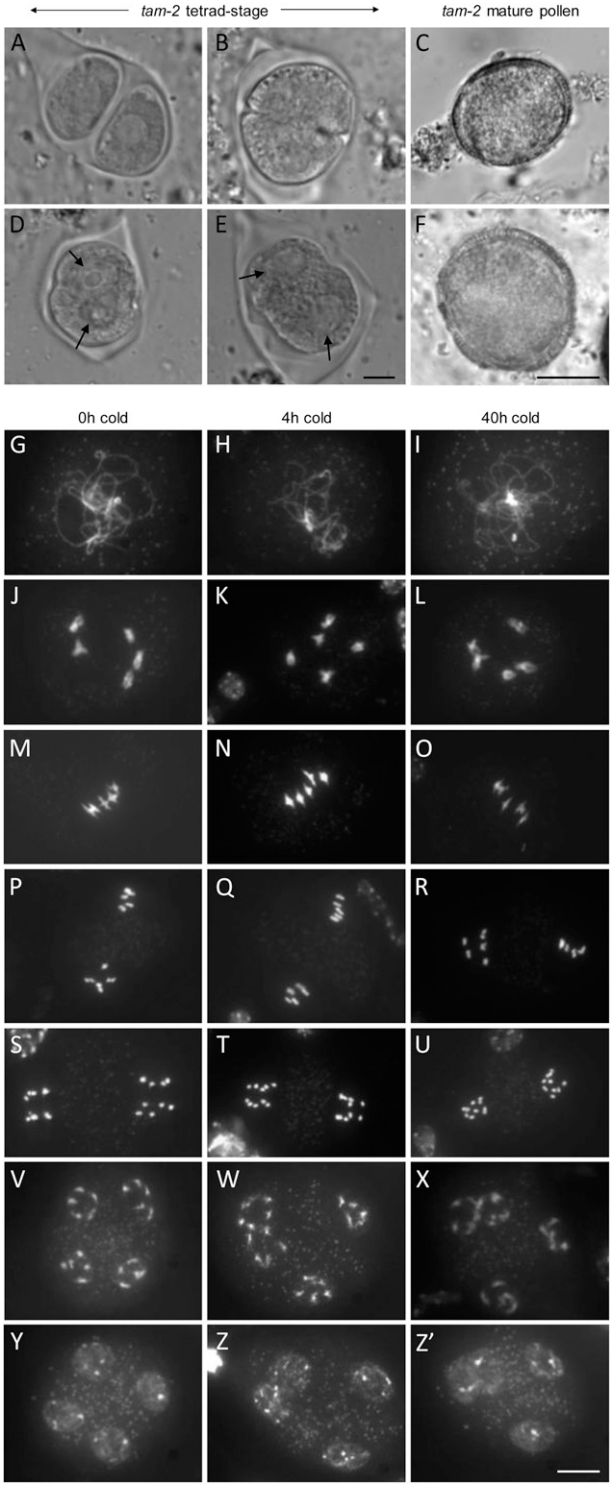

Figure 5. Cold-stressed male meiocytes show a regular prophase I and reductional chromosome division. A to F, Tetrad-stage *tam-2* male meiocytes under control conditions (A; dyads) and 1 d post cold shock (40 h, 4°C–5°C; B, D, and E) and representative images of a mature diploid *tam-2* pollen grain under normal growth conditions (C) and an enlarged spore at 7 d post cold shock treatment (F). Arrows indicate the restituted 2n nuclei in *tam-2* tetrad-stage meiocytes. G to Z′, DAPI-stained chromosome spreads of nontreated (G, J, M, P, S, V, and Y) and 4-h (H, K, N, Q, T, W, and Z) and 40-h (I, L, O, R, U, X, and Z′) cold-stressed Arabidopsis male meiocytes at different stages in the meiotic cell division: pachytene (G–I), diakinesis (J–L), metaphase I (M–O), metaphase II (P–R), anaphase II (S–U), telophase II (V–X), and tetrad stage (Y–Z′). Bars = 10 μm.

formation of chiasmata (physical crossover points) and bivalents in prophase I (Fig. 5, J–L), and the segregation of homologous chromosomes and sister chromatids in MI (Fig. 5, M–O) and MII (Fig. 5, P–U), respectively, appeared normal, indicating that cold stress does not affect meiotic chromosome segregation (e.g. spindle biogenesis and functionality) and thus typically generates four haploid sets of five chromosomes at the end of MII (Fig. 5, V–X). In the final step of meiosis, however, cold-stressed meiocytes occasionally showed structural aberrations in the telophase II cellular configuration. In contrast to nontreated telophase II meiocytes, which typically show a distinct organelle band between all four haploid nuclei (Fig. 5, V and Y), cold-stressed meiocytes often lacked one or more of these internuclear organelle structures and had two or more haploid nuclei colocalized (Fig. 5, W, X, Z, and Z′).

Thus, although low temperatures do not interfere with meiotic chromosome segregation processes, cold stress appears to affect the proper deposition and/or maintenance of the meiotic organelle band at the end of MII. As these internuclear organelle structures predefine the position of the meiotic cell plate, these observations support the hypothesis that cold stress specifically affects one or more processes involved in postmeiotic cytokinesis and/or cell wall formation.

Cold Stress-Induced Defects in Postmeiotic Cytokinesis Are Due to Alterations in Radial Microtubule Array Organization

To characterize the cold-induced defects in postmeiotic cell plate formation, we stained cell plates from Arabidopsis meiocytes 20 to 24 hpt using aniline blue. Under normal conditions, the four spores of a male meiotic tetrad are isolated by a centripetally oriented, X-shaped callosic cell plate (Fig. 6C). One day after cold treatment, however, this postmeiotic cell plate configuration appeared altered and often displayed major irregularities. In contrast to the quadripolar infurrowing in normal postmeiotic cytokinesis (Fig. 6A), cold-stressed meiocytes generally exhibited only two or three sites of active infurrowing (Fig. 6B) and consequently generated a single bipolar or a T-shaped tripolar cell plate at the end of MII (Fig. 6, D–H). Moreover, although most cold-stressed cell plates displayed a proper connection to the cell periphery, some appeared deflected and mislocalized and did not properly connect to the cell wall (Fig. 6F). In addition, cell plates in both mature and immature cold-stressed meiocytes appeared thinner and showed less staining intensity, indicating that the integrity of the newly

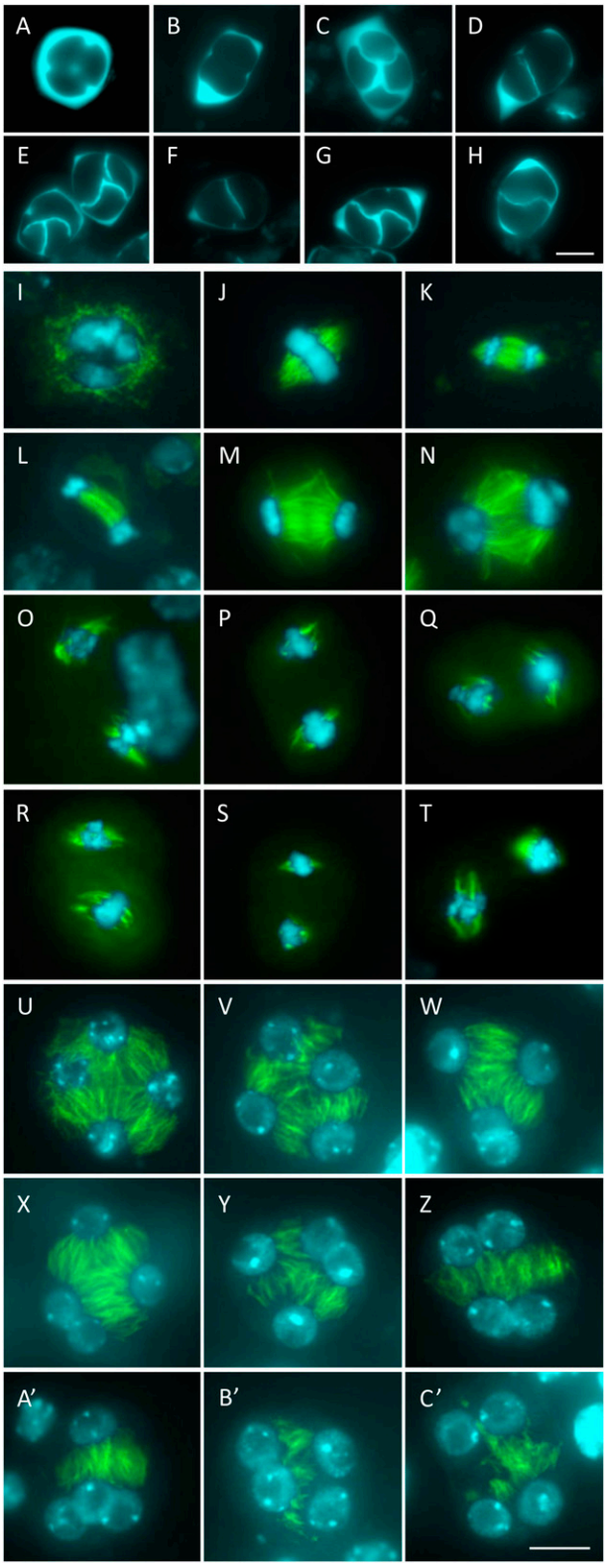

Figure 6. Cold stress-induced defects in postmeiotic cell plate formation are due to alterations in RMA formation. A to H, Aniline blue staining of callose in precytokinetic (A and B) and mature (C–H) meiocytes under control conditions (A and C) and upon cold treatment (B [20 hpt] and D–H [24 hpt]). Bar = 20 μm. I to C′, Tubulin-α immunolocalization of cold-shocked male meiocytes (0 hpt; 40 h at 4°C–5°C) at different stages in the meiotic cell cycle: diakinesis (I), metaphase I (J), anaphase I (K), telophase I (L), MI-MII interphase (M and N), metaphase II (O–T), and telophase II (U–C′). For both the metaphase II and the telophase II stages, an untreated control meiocyte was included as a reference (O and U, respectively). Tubulin-α is shown as green and DAPI is shown as cyan. Bar = 5 μm.

formed cell plate was compromised. From this, we conclude that cold stress interferes with the proper biogenesis and/or delivery of callose at the equatorial division plane.

Because callose and other cell plate components are deposited at the division planes by a network of microtubule (MT) arrays, we examined the integrity and the localization of MT structures at 0 and 4 hpt using tubulin-α immunocytology. Except for the tetrad stage, which showed clear alterations in MT organization, all other meiotic stages exhibited a normal MT distribution pattern, similar to nonstressed meiocytes (Fig. 6, I–T). In agreement with the regular meiotic chromosome segregation observed in earlier experiments (Fig. 5, G–X), we found that cold-stressed male meiocytes generate a proper internuclear phragmoplast at the end of telophase I (Fig. 6, M and N) and a normal single (Fig. 6, J and K) and double (Fig. 6, O–T) bipolar spindle structure at metaphase I and II, respectively. At telophase II, however, the microtubular cytoskeletal organization appeared altered.

Under normal growth conditions, telophase II male meiocytes typically generate a MT network that consists of six tetrahedrally arranged phragmoplast-like structures, which are localized between the four haploid nuclei (Fig. 6U). These MT structures, generally termed radial microtubule arrays (RMAs), are essential for postmeiotic cell plate formation (Peirson et al., 1997), as they constitute a physical barrier between the meiotic nuclei and mediate the accumulation of vesicles and cell wall components at the developing cell plate (Otegui and Staehelin, 2004). Although cold-stressed tetrads (during cold and 4 hpt) always displayed a proper tetrahedral positioning of the four haploid nuclei, formation of the cytokinetic RMA network often appeared severely altered and typically displayed asymmetric MT arrays or a complete omission of one or more internuclear phragmoplast-like structures (Fig. 6, W–C′; Supplemental Fig. S3). These cold-induced RMA alterations appeared randomly distributed and generated meiotic tetrads with only one, two, or three intact phragmoplast-like structures. In some cases, male meiocytes also exhibited a decreased number of MT fibers between the four meiotic nuclei (Fig. 6, B′ and C′), suggesting that cold stress directly affects MT polymerization and/or bundling. We also found that cold-stressed tetrads with defects in RMA structure generally contained two or three nuclei that were in close proximity to each

other (Fig. 6, W–A′). Since the position of the nuclei directly coordinates RMA formation in meiotic tetrads, the cold-induced colocalization of two or more nuclei at telophase II could be the primary cause of the defects in RMA formation. However, as meiotic spindle structure and positioning were not affected by cold and defects in RMA organization were also observed between distantly located nuclei (Fig. 6, Y and C′), postmeiotic nuclear colocalization is most likely a direct consequence of defects in RMA formation and not vice versa. Collectively, these data demonstrate that a short period of cold stress in Arabidopsis male meiosis specifically disrupts postmeiotic RMA formation and/or stability and leads to alterations in internuclear organelle band formation and callose deposition and the eventual loss of postmeiotic cell plate formation. Moreover, since telophase II RMA defects were not only observed during cold but also upon transfer to normal growing temperatures (e.g. 4 h post cold treatment; Supplemental Fig. S3), we conclude that alterations in telophase II RMA organization are not recovered under warm conditions and, by consequence, significantly delay the progression of the meiocyte's developmental program. This developmental delay explains why defects in postmeiotic cell plate formation are only observed 22 to 26 h post cold treatment and not during the first hours upon transfer to normal conditions (under normal conditions, progression from telophase II to the tetrad stage generally takes 6–12 h).

Cold-Induced Cytokinetic Defects in Meiosis Are Not Regulated by MKK2

Male-specific meiotic cytokinesis and the formation of RMAs in Arabidopsis is regulated by a distinct MAPK signaling pathway, linking TES/STUD/AtNACK2, AtANP3, AtMKK6/ANQ1, and AtMPK4 together in a cascade that modulates the downstream activity of MT-binding proteins (Takahashi et al., 2010). Although MPK4 phosphorylation and the activation of cytokinesis is regulated by MKK6, it was recently shown that MPK4 can also be activated by MKK2 (Teige et al., 2004). As MKK2 is a signaling kinase involved in cold stress perception, we hypothesized that the cold stress-induced phosphorylation of MPK4 through MKK2 might initiate the premature, and thus altered, formation of postmeiotic RMA structures, bypassing the developmentally regulated activation through TES. To test this hypothesis, cold-induced binuclear and polynuclear microspore formation was monitored in two mutant alleles of *MKK2*: *mkk2*-SALK$^{-/-}$, which retains 29.0% residual expression (data not shown), and *mkk2*-SAIL$^{-/-}$, which is a null allele (Teige et al., 2004). Upon cold shock, we found that both *mkk2*$^{-/-}$ alleles produced significant numbers of binuclear and polynuclear microspores 1 d after treatment, similar to the levels observed in a wild-type background (Table II). Based on this finding, we conclude that MKK2 does not modulate the cold stress sensitivity of postmeiotic cell plate formation.

Although mutations in *TES/STUD/AtNACK2* were reported to completely omit cytokinesis in male meiosis, generating enlarged tetranuclear microspores without any cell plate (Fig. 7, A, E, and I; Spielman et al., 1997), we observed that *tes-4*$^{-/-}$ occasionally forms partial or complete cell plates at the end of male MII (Fig. 7, F–H and J–L) and generates *qrt1*$^{-/-}$-like dyad- and triad-shaped microspores (Fig. 7, B–D). Since these defects are identical to the alterations observed in cold-stressed wild-type male meiocytes, we hypothesized that the expression and/or function of TES or one of the downstream cytokinesis-specific MAPK signaling factors (e.g. MKK6 or MPK4) is affected under cold stress conditions. To test this hypothesis, we monitored the expression of major MAPK signaling components in flower buds before and after cold treatment using quantitative reverse transcription (qRT)-PCR. For all three kinases tested (MPK4, MKK6, and TES), we found either no change or a non-significant decrease in expression 0 and 4 h after cold treatment (Fig. 7M), indicating that cold stress does not significantly affect transcription of the major MAPK signaling proteins involved in postmeiotic cytokinesis.

Table II. *Cold-induced binuclear and polynuclear microspore formation in Arabidopsis mkk2 mutants*

Frequency of binuclear and polynuclear microspore formation is shown in the wild type (Columbia-0 and Wassilewskija) and two *MKK2* T-DNA insertional mutants 30 h post cold treatment (40 h at 4°C–5°C). Statistical comparison was performed using one-way ANOVA (α = 0.05, Tukey's post hoc test).

Sample	*n*	Value	Microspore Frequency			
			Uninuclear	Binuclear	Trinuclear	Tetranuclear
			%			
Control, Columbia-0	2,857	Mean	93.1	6.0	0.8	0.1
		SD	7.0	5.7	1.7	0.2
mkk2-SALK	3,127	Mean	93.2	6.1	0.5	0.1
		SD	6.5	5.5	1.1	0.3
Control, Wassilewskija	1,884	Mean	90.8	8.8	0.3	0.1
		SD	11.2	10.8	0.4	0.1
mkk2-SAIL	1,391	Mean	93.4	6.1	0.5	0.0
		SD	4.9	4.0	0.9	0.0

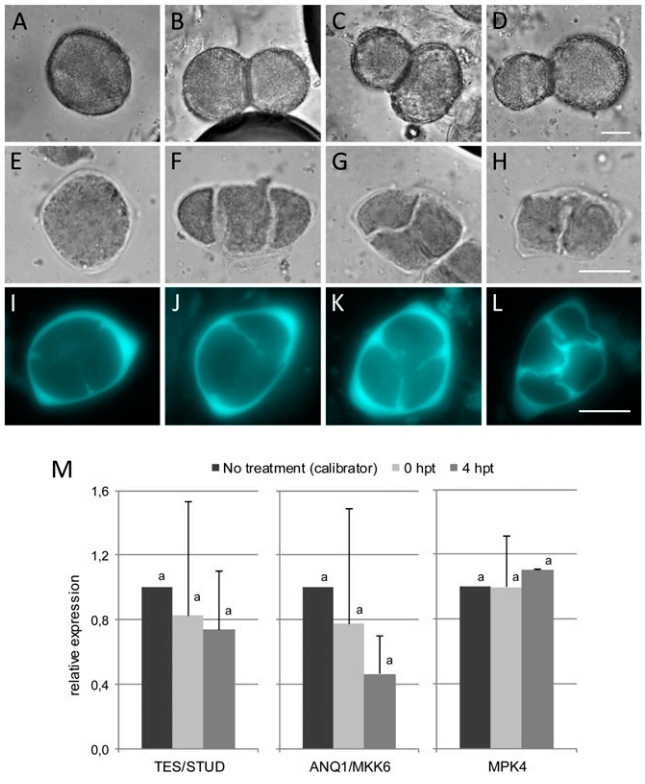

Figure 7. Arabidopsis *tes-4* microsporogenesis phenocopies cold-induced defects in male meiotic cell plate formation. A to D, Pollen isolated from the Arabidopsis *tes-4*$^{-/-}$ mutants are normally fully restituted (A) but sometimes show Qrt1^{-}-like dyad configurations, indicating partial cytokinesis (B–D). E to H, Orcein staining of the *tes-4*$^{-/-}$ tetrad stage generally shows a complete loss of cell wall establishment with the formation of monads (E), but occasionally dyads and triads are observed (F–H). I to L, Aniline blue staining of *tes-4*$^{-/-}$ meiocytes. Although generally no callosic cell plates are observed (I), *tes-4*$^{-/-}$ meiocytes sometimes show partial and/or complete cell walls (J–L). Bars = 10 μm. M, Relative expression of *TES/STUD*, *ANQ1/MKK6*, and *MPK4* in meiotic flower buds (stages 8–10) 0 and 4 h after cold shock treatment (40 h, 4°C–5°C). [See online article for color version of this figure.]

However, as meiocyte-specific changes in transcription can be masked or attenuated by the expression in surrounding tissues, no clear conclusions can be made about the effect of cold stress on the expression of TES and other MAPK signaling components involved in postmeiotic cytokinesis.

DISCUSSION

Cold Stress Generates Diploid and Polyploid Gametes by RMA-Based Defects in Postmeiotic Cell Plate Formation

In this study, we show that short periods of cold stress (1–40 h at 4°C–5°C) in flowering Arabidopsis plants induce restitution of the male meiotic cell division, leading to the formation of diploid, triploid, and tetraploid spores. Based on cytological observations, we found that short periods of low temperature specifically disrupt the organization and/or maintenance of the telophase II-specific internuclear RMAs, without affecting the segregation of meiotic chromosomes, and induce defects in internuclear organelle localization and callose deposition at the end of MII, typically leading to (partial) defects in postmeiotic cell plate formation and delaying the developmental progression of the meiocyte upon transfer to normal conditions (Fig. 8). As nuclei of the resulting binuclear and polynuclear spores spontaneously fuse before the first mitotic pollen division, cold-induced defects in postmeiotic cell plate formation were found to yield viable diploid and polyploid pollen grains 6 to 8 d post cold treatment. Moreover, since cold-induced dyads and triads predominantly contain SDR-type 2n gametes, the defect in meiotic cell plate formation typically generates diploid spores with a high level of homozygosity, particularly at the genomic regions close to the centromere. As such, these findings are particularly relevant for enhancing our understanding of how polyploidization may occur in natural populations and how it may be influenced by environmental factors such as temperature stress. Moreover, the characterization of cold stress-induced 2n gamete formation may suggest simple strategies for plant breeding programs that include polyploidization or reverse breeding (Dirks et al., 2009; Wijnker et al., 2012).

In this study, we demonstrate that cold stress-induced defects in Arabidopsis postmeiotic cell plate formation are caused by alterations in the biogenesis and/or stability of the telophase II RMAs, internuclear phragmoplast-like MT arrays that are essential for postmeiotic cell wall formation. In general, MTs are known to be extremely temperature sensitive, displaying a quick depolymerization under the influence of adverse temperatures (Brinkley and Cartwright, 1975; Okamura et al., 1993). In line with this, several studies have reported the detrimental influence of heat and cold stress on the biogenesis and stability of the cortical MT array and cytoskeletal figures in somatic cells (Carter and Wick, 1984; Smertenko et al., 1997; Orvar et al., 2000; Gupta et al., 2001; Magnard et al., 2001; Abdrakhamanova et al., 2003). Several studies (mostly in animal species) have additionally demonstrated that, among cytological figures, the metaphase-specific spindle structure, both in mitotic and meiotic cell division, is particularly sensitive to reduced temperature environments (Magistrini and Szöllösi, 1980; Wang et al., 2001). Although under certain conditions this cold-induced loss of spindle formation can be recovered upon rewarming, defective spindle figures generally lead to a block in cell division or aberrations in chromosome segregation, inducing cell cycle arrest and/or aneuploidy, respectively (Aman and Parks, 1994; Wang et al., 2001; Liu et al., 2003; Suzuki et al., 2007). In contrast to these findings, we here demonstrate that Arabidopsis male

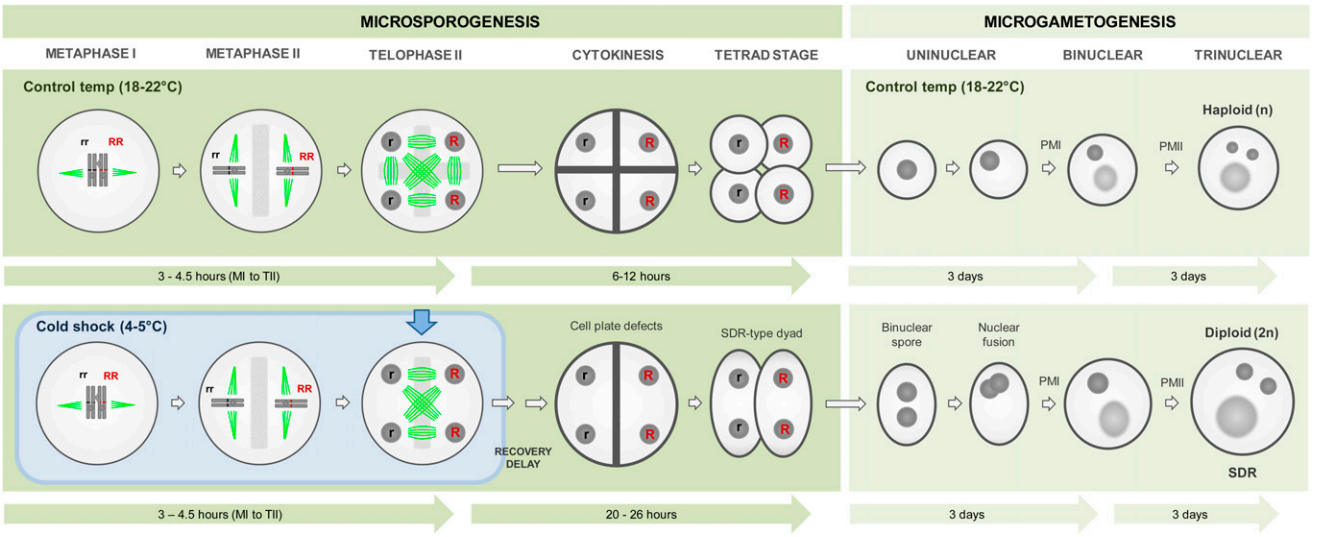

Figure 8. Schematic representation of the stage-specific sensitivity of Arabidopsis male meiosis to short periods of low temperature (RMA formation and/or stability) and the associated formation of SDR-type 2n spores.

meiocytes, under low-temperature stress (e.g. 4°C–5°C), do not exhibit MT depolymerization and show normal cytoskeletal MT arrangements (including normal spindles in metaphase I and II) from prophase I to metaphase II, indicating that cold does not significantly affect the biogenesis and/or stability of MTs in the process of meiotic chromosome segregation. Moreover, as we never observed any defect in meiotic chromosome segregation (e.g. lagging chromosomes or aneuploidy) and cold-stressed meiosis always resulted in four distinct nuclei each containing the haploid number of five chromosomes, we conclude that short periods of chilling do not significantly affect spindle biogenesis and/or functionality in Arabidopsis male meiosis. The cold-induced formation of meiotically restituted diploid and polyploid gametes, therefore, is not caused by alterations in spindle morphogenesis. In the final stage of the meiotic cell cycle, at telophase II, however, clear defects in internuclear MT array organization (RMA) were detected upon exposure to low-temperature stress. As the frequency and structure of these RMA defects (telophase II) strongly correlate with the defects in postmeiotic cell plate formation (tetrad stage), and as similar postmeiotic cytokinetic defects in the RMA-deficient Arabidopsis *tes* and *mpk4* mutants were shown to generate multinuclear spores, we conclude that cold-induced binuclear and polynuclear spore formation is directly caused by alterations after meiotic RMA formation. Moreover, since observations in meiotic spindle-defective mutants (e.g. *mps1* and double heterozygous *AtKIN14a/atkin14a AtKIN14b/atkin14b*) have demonstrated that defects in MI or MII spindle structure do not affect postmeiotic cell plate formation (Quan et al., 2008; Jiang et al., 2009), we can exclude the possibility that cold-induced defects in postmeiotic RMA formation originate from slight (or maybe undetected) aberrations in MII spindle morphology. On the other hand, we cannot exclude the possibility that some cold-induced meiotic restitution events on rare occasions may directly originate from aberrations in spindle positioning, as already observed in heat-stressed rose meiocytes (e.g. through parallel spindle formation; Pécrix et al., 2011).

In general, little is known about the effect of low-temperature stress on the microtubular organization and dynamics of the cytoskeletal figures (e.g. spindles, perinuclear arrays, and RMAs) in the meiotic cell division. In line with our observations, Danilchik et al. (1998) found that in *Xenopus laevis* female meiosis, short periods of cold depolymerize cytokinetic MT and prevent the addition of new plasma membrane to the cleavage plane, causing furrows to recede. Tang et al. (2011) recently reported that cold-induced male sterility in a wheat thermosensitive genic male-sterile line is caused by defects in MT phragmoplast formation and cell plate assembly at MI, which leads to a premature abortion of the developing pollen mother cells. These findings, together with our observations, suggest that the cold sensitivity of MT cytoskeletal figures in meiosis significantly varies from MT structures in mitosis, with the internuclear precytokinetic phragmoplast-like RMA structure being the most sensitive MT structure in meiosis compared with the spindle in mitosis. In line with this, tissue-specific differences in the microtubular response to cold have already been found in different cell types in the maize root apex (Baluska et al., 1993).

In the wheat thermosensitive genic male-sterile line, cold-induced defects in MT phragmoplast and MI cell plate formation are caused by an aberrant

localization and biogenesis of F-actin filaments (Xu et al., 2012). Since actin microfilaments mediate trafficking of vesicles and organelles and thereby regulate endomembrane dynamics during de novo cell plate formation, these proteins are considered essential for MT phragmoplast establishment and associated cell plate formation (Valster et al., 1997; Endlé et al., 1998; Collings et al., 2003; Higaki et al., 2008). Hence, cold-induced defects in postmeiotic RMA formation in Arabidopsis may be caused by alterations in meiotic actin scaffolding and/or microfilament stability. In support of this hypothesis, similar defects in meiotic cell plate formation were observed in mutant forms of Arabidopsis FORMIN14 (AFH14), a type II formin that links MT and microfilament (Li et al., 2010). Since loss of AFH14 function induces the formation of dyads and triads through defects in RMA assembly, actin filaments are considered essential for postmeiotic RMA organization/stability and, therefore, may be implicated in cold-induced meiotic restitution. However, due to the complex interplay between actin and microtubuli during the process of cell plate formation (Jürgens, 2005; Sano et al., 2005; Petrásek and Schwarzerová, 2009), it is difficult to pinpoint the exact cytological basis for cold-induced defects in meiotic cytokinesis in the wheat thermosensitive genic male-sterile and Arabidopsis male meiocytes.

Besides defects in actomyosin scaffolding, cold-induced defects in Arabidopsis postmeiotic cell plate formation could also originate from altered positioning of haploid nuclei at the end of MII. Although haploid nuclei appeared properly positioned in a wild-type-like tetrahedral conformation, cold-stressed Arabidopsis meiocytes often displayed two or three nuclei in closer proximity, potentially hindering the proper formation of internuclear RMA structures. Disruption of internuclear RMAs through altered positioning of telophase II nuclei has already been observed in the conditional Arabidopsis mutant *radially swollen4* (*rsw4*; Yang et al., 2009). *RWS4* encodes the caspase-like separase AtESP (Wu et al., 2010), a protease that cleaves sister chromatid-specific cohesin complexes at the onset of anaphase (Liu and Makaroff, 2006). Loss of AtESP function causes chromatid nondisjunction and leads to a partial loss of internuclear RMA formation at the end of MII (Yang et al., 2011), suggesting that alterations in chromosome segregation and postmeiotic nuclear positioning can lead to aberrations in RMA formation. Similarly, in animal meiocytes (e.g. human oocytes), exposure to low temperatures has been found to induce depolymerization of the spindle microtubuli (Wang et al., 2001), leading to a nondisjunction of chromatids at MII and the formation of polyploid and aneuploid embryos in the next generation (Van der Elst et al., 1988; Pickering et al., 1990; Almeida and Bolton, 1995). However, as no defects in meiotic chromosome segregation and spindle formation were observed in cold-stressed Arabidopsis male meiocytes, and as altered RMAs were also found between distantly located telophase II nuclei, we conclude that cold-induced defects in postmeiotic cell wall establishment were not caused by alterations in meiotic chromosome segregation or telophase II nuclear positioning but rather by an alteration of the internuclear RMA structure.

Evolutionary Implications of Cold-Induced 2n Gamete Formation

In Arabidopsis, cold-induced defects in meiotic cell plate formation predominantly lead to the formation of 2n gametes. Based on FTL dyad/triad genotyping and *atspo11-1-3*$^{-/-}$ tetrad-stage analysis, we found that the majority of these meiotically restituted 2n spores are genetically equivalent to SDR and thus have the potential to produce highly homozygous progeny plants. In addition to the SDR-type 2n gametes, cold stress also generates a subset of dyads and triads that contain FDR-type 2n spores. FTL marker analysis revealed that up to one-fifth of the dyads contain heterozygous FDR-like 2n spores. Although some FDR-type spores may arise from a meiotic SDR-type restitution accompanied by recombination, tetrad-stage analysis in the *atspo11-1-3*$^{-/-}$ background demonstrates that at least some 2n spores are generated through an FDR-type restitution.

In plant evolution, new polyploid species are often thought to arise from diploid progenitors that spontaneously produce 2n gametes (Bretagnolle and Thompson, 1995). However, despite its evolutionary relevance, little is known about the genetic constitution of 2n gametes, and it is unclear whether FDR or SDR types have contributed to the formation of established polyploids. In theory, FDR 2n gametes have an adaptive advantage over SDR 2n gametes because they confer a high level of heterozygosity to their progeny (Peloquin, 1983; Hermsen, 1984; Carputo et al., 2003; Peloquin et al., 2008). The increased genotypic diversity and augmented proportion of triallelic and tetraallelic genotypes in FDR-generated polyploids typically lead to a lower coefficient of inbreeding in the progeny compared with SDR-directed polyploidization (Watanabe et al., 1991).

From that point of view, the predominant formation of SDR-type 2n gametes upon cold stress would be evolutionarily less beneficial. However, since we additionally found that recombination still occurs under low-temperature conditions, cold-induced SDR-type 2n gametes have significant levels of genomic heterozygosity toward the telomeres. As a result, cold-induced SDR 2n gametes can provide some heterozygosity and associated allelic diversity to its polyploid progeny. Moreover, as most natural polyploid lineages are thought to originate from a unilateral polyploidization event, in which the fusion of reduced and unreduced gametes results in the formation of unstable triploid intermediates (triploid bridge hypothesis; Yamauchi et al., 2004; Considine et al., 2012), the genetic influence of both types of 2n gametes on the

evolutionary success of the resulting polyploid is less relevant and depends more on the fitness of the triploid intermediate.

In plant evolution, the induction of 2n gamete formation and associated plant polyploidization is either mediated by de novo mutations or is imposed by environmental (stress) conditions. Our results, together with the relatively high number of polyploid plant species in areas with extreme environments (Flovik, 1940; Stebbins, 1984; Guggisberg et al., 2006) and the notion that ancient polyploidization events often coincided with adverse climatic events (e.g. glaciation periods; Brochmann et al., 2004; Van de Peer et al., 2009), support the hypothesis that stress-induced formation of diploid gametes may have substantially contributed to plant polyploidization and associated speciation (Wood et al., 2009).

Molecular Regulation of Cold-Induced Meiotic Restitution?

Temperature stress in plants, as in other organisms, has been shown to alter the expression of cell cycle regulators. In maize leaves, for example, long-term exposure to low night temperatures was found to change the expression of several cell cycle-related genes (e.g. *CYCA3;1*), leading to a significant prolongation of mitotic cell cycle duration (Rymen et al., 2007). In addition, Bita et al. (2011) recently demonstrated that short periods of moderate heat stress cause a general down-regulation of gene expression in the anthers of a heat-sensitive tomato (*Solanum lycopersicum*) line, providing evidence that meiosis-specific transcription also responds to temperature stress.

Although it is unclear whether short periods of chilling can modulate the expression of meiotic genes, our data suggest that the cold stress-induced restitution of male meiosis and the associated formation of diploid and polyploid spores is not caused by an alteration of meiotic cell cycle regulation (e.g. *OSD1* or *TAM/CYC1;2*) but instead putatively results from an altered regulation of genes/transcripts/proteins involved in postmeiotic cell plate formation. In support of this hypothesis, similar defects in postmeiotic cell plate formation have already been documented in some Arabidopsis mutants grown under normal conditions (Spielman et al., 1997; Soyano et al., 2003; Li et al., 2010; Zeng et al., 2011).

For example, Arabidopsis *afh14*$^{-/-}$ mutants were found to display similar aberrations in meiotic RMA formation and, by consequence, also form restituted dyads and triads that contain binuclear spores (Li et al., 2010). In contrast to cold-induced meiotic restitution, however, *afh14-1*$^{-/-}$ produces parallel spindles at metaphase II (more than 50%) rather than the perpendicularly oriented ones observed in wild-type meiosis. As this cytological mechanism of meiotic restitution typically generates dyads and triads that contain FDR-type 2n gametes (d'Erfurth et al., 2008; De Storme and Geelen, 2011) and not the SDR-type gametes observed in cold-stressed microsporogenesis, we conclude that cold-induced meiotic restitution in plants is not regulated by AFH14.

Functional loss of the cytokinetic MAPK signaling components (TES/STUD, ANQ/MKK6, and MPK4) induce a complete failure of cytokinesis in Arabidopsis male meiosis (Spielman et al., 1997; Soyano et al., 2003; Zeng et al., 2011). However, as partial postmeiotic cell plates and *qrt1*$^{-/-}$-like tetrad- and dyad-shaped pollen, two phenotypes typical for cold-induced meiotic restitution, were observed in *tes-4*$^{-/-}$ (this study) and *anq1*$^{-/-}$ male sporogenesis (Soyano et al., 2003), we hypothesize that TES/STUD kinesin or the downstream MAPK signaling components may play a role in the cold stress-induced formation of diploid and polyploid pollen. By analyzing Arabidopsis mutants, we demonstrated that cold-induced defects in meiotic cell plate formation are not mediated by MKK2, a MAPK signaling protein that potentially links cold stress to MPK4-mediated cytokinesis (Teige et al., 2004). Moreover, in contrast to wheat thermosensitive genic male-sterile male meiocytes, which show a transcriptional change of cytoskeletal signaling components upon cold stress (Tang et al., 2011), no significant changes in the expression of major cytokinesis-specific MAPK signaling components were observed in our study. However, as meiosis-specific transcriptional changes can be masked by expression in surrounding tissue, and as (post)translational modifications were not assessed, we cannot exclude the possibility that low temperatures affect the regulation of the postmeiotic cytoskeletal MAPK signaling pathway and consequently induce defects in meiotic cell plate formation. In order to test this, more detailed tissue-specific analyses have to be performed.

MATERIALS AND METHODS

Plant Materials and Growth Conditions

Arabidopsis (*Arabidopsis thaliana*) Columbia-0 and Wassilewskija wild-type accessions were obtained from the Nottingham Arabidopsis Stock Centre. The FTL reporter lines in the *qrt1-2*$^{-/-}$ background (FTL 3253, FTL 1273, and I4a), used for genotyping 2n gametes, were described earlier (Berchowitz and Copenhaver, 2008). The *mkk2-SAIL* T-DNA insertion line (Garlic_511_H01.b.1a.Lb3Fa) was donated by M. Teige, and the meiotic mutants *atspo11-1-3* (SALK_146172) and *tam-2* (SAIL_505-C06) were kindly provided by R. Mercier. The other mutants used in this study, namely *mkk2-SALK* (FLAG_629G03) and *tes-4* (N9353; Wassilewskija background; Spielman et al., 1997), were obtained from the European Arabidopsis Stock Centre. For the in vivo gametophytic ploidy analysis, Arabidopsis plants harboring *pMGH3::H2B-GFP* (provided by D. Twell) and *pWOX2::CENH3-GFP* (De Storme and Geelen, 2011) were used.

Following in vitro seed germination (6–8 d; K1 medium), seedlings were transferred to soil and cultivated in growth chambers at 12 h day/12 h night, 20°C, and less than 70% humidity. Upon flowering, the photoperiod was changed to a 16-h-day/8-h-night regime. For cold shock, flowering plants

were transferred to a cold climate chamber (4°C–5°C) for different time periods (1, 2, 4, 20, or 40 h). After cold treatment, plants were returned to normal growth conditions.

Cytology

Pollen DNA staining was performed as described earlier with minor modifications (Durbarry et al., 2005). After pollen extraction in 0.5 M EDTA, the resulting pollen pellet was fixed in 3:1 ethanol:acetic acid for 30 min, washed with distilled water, and resuspended in DAPI solution (1 μg mL^{-1}; Sigma) for 30 min. Subsequent centrifugation and additional washing steps resulted in a clear, DAPI-stained pollen sample.

Analysis of the male meiotic outcome (tetrad-stage analysis) was performed by selecting meiotic buds based on size and shape (floral bud stage 9; 0.3–0.4 mm; Armstrong and Jones, 2003) and squashing them on a slide in a drop of 4.5% (w/v) lactopropionic orcein solution. Similarly, callose cell wall staining of male meiotic products was performed by squashing stage 9 flower buds in a drop of aniline blue solution (0.1% [m/v] in 0.033% K_3PO_4 [m/v]). Buds producing significant numbers of fully developed meiotic products were used for counting and monitoring assays. Analysis of nuclear configurations in tetrad-stage meiocytes and developing microspores was performed by releasing spores in a drop of acetocarmine solution (0.45% [m/v] in distilled water). Visualization of microspore- and pollen-specific GFP-labeled reporter constructs was optimized by squashing buds in a 0.05 M $NaPO_4$ (pH 7.0) and 0.5% Triton X-100 (v/v) solution. Male meiotic chromosome spreads were prepared according to the protocol described (De Storme and Geelen, 2011). To avoid changes in meiotic chromosome behavior in cold-stressed meiocytes, the isolation and fixation of Arabidopsis flower buds was directly performed in the cooling chamber using a cold fixation buffer (4°C–5°C).

Tetrad-Based 2n Gamete Genotyping

The genotypic characterization of 2n male gametes was performed using heterozygous FTL markers in the *qrt1-2*$^{-/-}$ background. To obtain *qrt1-2*$^{-/-}$ plants heterozygous for the FTL marker, two differently labeled homozygous FTL lines in the *qrt1-2*$^{-/-}$ background were intercrossed. Resulting progeny were used for genotypic characterization of cold stress-induced meiotically restituted 2n gametes. Upon cold shock, mature *qrt1-2*$^{-/-}$ FTL$^{+/-}$ flowers were isolated 6 to 8 dpt and tapped in a droplet of distilled water. Segregation of the fluorescent signal in dyads and triads was monitored using an Olympus IX81 fluorescence microscope.

In restituted dyads, sister chromatids with the FTL marker either disjoin, generating full fluorescent dyads (m−/m−; FDR type), or cosegregate to yield dyads with one fluorescent spore (mm/–; SDR type). Similarly, segregation of the heterozygous FTL marker can be used to genotype triad-specific 2n spores. If the fluorescent signal is confined to, or absent in, the larger 2n spore, sister chromatids have cosegregated (mm/−/− or –/m/m; SDR type). If the marker is present in both the haploid and the diploid gamete, FTL-containing sister chromatids have disjoined (m−/m/−; FDR type).

Tubulin Immunolocalization

To analyze microtubular structures and postmeiotic RMA organization in male sporogenesis, an α-tubulin immunolocalization assay was performed using the method of Mercier et al. (2001) with minor modifications. After *m*-maleimidobenzoyl *N*-hydrosuccinimide ester treatment (100 μM in 50 mM potassium phosphate buffer and 0.05% [v/v] Triton X-100, pH 8; 30 min under vacuum) and fixation in 4% (w/v) paraformaldehyde, inflorescences were washed in 50 mM potassium phosphate buffer (pH 8) and digested in an enzyme mixture consisting of 0.3% (w/v) pectolyase (Sigma), 0.3% (w/v) cytohelicase (Sigma), and 0.3% (w/v) cellulase (Sigma) in a humid chamber at 37°C. Enzyme-digested anthers were dissected, squashed, and fixed on a slide by freezing in liquid nitrogen. Released cells were then immobilized with a thin layer of 1% (w/v) gelatin, 1% (w/v) agarose, and 2.5% (w/v) Glc and digested for 30 min at 37°C with the same enzyme mix. After rinsing with potassium phosphate buffer, immobilized cells were incubated overnight at room temperature with rat α-tubulin primary antibody (0.3% [v/v]; clone B-5-1-2; Sigma-Aldrich) in phosphate-buffered saline, 0.1% (v/v) Triton X-100, and 4.5 g L^{-1} bovine serum albumin. Cells were rinsed three times with phosphate-buffered saline and treated for 5 h with 0.5% (v/v) secondary antibody (labeled goat anti-rat) at 37°C in the dark. After five phosphate-buffered saline rinses, a small droplet of DAPI (2 μg mL^{-1}) in Vectashield mounting medium (Vector Laboratories) was added. To avoid potential recovery of cold-stressed meiotic cytoskeletal figures upon transfer to normal temperature conditions, the first steps of the tubulin immunolocalization protocol (e.g. *m*-maleimidobenzoyl *N*-hydrosuccinimide ester treatment and fixation) were performed in the cooling chamber using cooled buffers (4°C–5°C).

Microscopy

Both bright-field and fluorescence microscopy were performed using an Olympus IX81 inverted fluorescence microscope equipped with an X-Cite Series 120Q UV lamp. Images were captured using an Olympus XM10 camera. Bifluorescent images and *Z*-stacks were processed using ImageJ. Confocal three-dimensional imaging of centromeric CENH3-GFP in developing microspores and pollen was performed using a Nikon A1r laser scanning microscope equipped with Axiovision software (LiMiD). Brightness settings were adjusted globally on some images using ImageJ.

Expression Analysis

Early flower bud and mature leaf RNA was prepared using the RNeasy Plant Mini Kit with additional on-column DNaseI treatment (Qiagen). First-strand cDNA was synthesized using the RevertAid H Minus cDNA Synthesis Kit (Fermentas) according to the manufacturer's guidelines. Quantitative gene expression analysis was performed by qRT-PCR on a Stratagene MX3000 real-time PCR system using the MAXIMA SYBR Green/ROX qPCR kit Master Mix (Fermentas). Sequences of primers used for specific amplification of MKK2, TES/STUD, ANQ1/MKK6, and MPK4, and housekeeping gene transcripts together with the corresponding qRT-PCR settings, are listed in Supplemental Table S3.

Supplemental Data

The following materials are available in the online version of this article.

Supplemental Figure S1. Cold shock induces restitution of male meiosis.

Supplemental Figure S2. Short cold shock induces restitution of male meiosis.

Supplemental Figure S3. Sustained RMA defects upon cold shock.

Supplemental Table S1. Frequency of large pollen upon cold shock.

Supplemental Table S2. Meiotic products in *atspo11-1-3*$^{+/-}$.

Supplemental Table S3. Quantitative PCR primers.

ACKNOWLEDGMENTS

We thank M. Teige (University of Vienna) and D. Twell (University of Leicester) for providing Arabidopsis seed material. Many thanks as well to M. Höfte and D. De Vleesschauwer (Phytopathology, University of Ghent) for technical advice regarding qRT-PCR. We are also grateful to R. Mercier and L. Cromer (Institut National de la Recherche Agronomique, Versailles) for demonstrating the tubulin immunolocalization protocol (STSM training supported by COST FA0903). We also thank W. De Vos and G. Meesen for their support in confocal microscopy (University of Ghent).

Received October 5, 2012; accepted October 24, 2012; published October 24, 2012.

LITERATURE CITED

Abdrakhamanova A, Wang QY, Khokhlova L, Nick P (2003) Is microtubule disassembly a trigger for cold acclimation? Plant Cell Physiol **44:** 676–686

Adams KL, Wendel JF (2005a) Novel patterns of gene expression in polyploid plants. Trends Genet **21:** 539–543

Adams KL, Wendel JF (2005b) Polyploidy and genome evolution in plants. Curr Opin Plant Biol **8:** 135–141

Almeida PA, Bolton VN (1995) The effect of temperature fluctuations on the cytoskeletal organisation and chromosomal constitution of the human oocyte. Zygote **3:** 357–365

Aman RR, Parks JE (1994) Effects of cooling and rewarming on the meiotic spindle and chromosomes of in vitro-matured bovine oocytes. Biol Reprod **50:** 103–110

Armstrong SJ, Jones GH (2003) Meiotic cytology and chromosome behaviour in wild-type Arabidopsis thaliana. J Exp Bot **54:** 1–10

Baluska F, Parker JS, Barlow PW (1993) The microtubular cytoskeleton in cells of cold-treated roots of maize (Zea mays L) shows tissue-specific responses. Protoplasma **172:** 84–96

Barata C, Hontoria F, Amat F, Browne R (1996) Demographic parameters of sexual and parthenogenetic Artemia: temperature and strain effects. J Exp Mar Biol Ecol **196:** 329–340

Beaton MJ, Hebert PDN (1988) Geographical parthenogenesis and polyploidy in Daphnia pulex. Am Nat **132:** 837–845

Berchowitz LE, Copenhaver GP (2008) Fluorescent Arabidopsis tetrads: a visual assay for quickly developing large crossover and crossover interference data sets. Nat Protoc **3:** 41–50

Bita CE, Zenoni S, Vriezen WH, Mariani C, Pezzotti M, Gerats T (2011) Temperature stress differentially modulates transcription in meiotic anthers of heat-tolerant and heat-sensitive tomato plants. BMC Genomics **12:** 384

Bogart JP, Elinson RP, Licht LE (1989) Temperature and sperm incorporation in polyploid salamanders. Science **246:** 1032–1034

Bretagnolle F, Thompson JD (1995) Tansley Review No. 78. Gametes with the somatic chromosome-number: mechanisms of their formation and role in the evolution of autopolyploid plants. New Phytol **129:** 1–22

Brinkley BR, Cartwright JJ Jr (1975) Cold-labile and cold-stable microtubules in the mitotic spindle of mammalian cells. Ann N Y Acad Sci **253:** 428–439

Brochmann C, Brysting AK, Alsos IG, Borgen L, Grundt HH, Scheen AC, Elven R (2004) Polyploidy in Arctic plants. Biol J Linn Soc Lond **82:** 521–536

Brownfield L, Hafidh S, Borg M, Sidorova A, Mori T, Twell D (2009) A plant germline-specific integrator of sperm specification and cell cycle progression. PLoS Genet **5:** e1000430

Brownfield L, Köhler C (2011) Unreduced gamete formation in plants: mechanisms and prospects. J Exp Bot **62:** 1659–1668

Carputo D, Frusciante L, Peloquin SJ (2003) The role of 2n gametes and endosperm balance number in the origin and evolution of polyploids in the tuber-bearing Solanums. Genetics **163:** 287–294

Carter JV, Wick SM (1984) Irreversible microtubule depolymerization associated with freezing-injury in Allium cepa root-tip cells. Cryo Lett **5:** 373–382

Coleman AW, Goff LJ (1985) Applications of fluorochromes to pollen biology. I. Mithramycin and 4′,6-diamidino-2-phenylindole (DAPI) as vital stains and for quantitation of nuclear DNA. Stain Technol **60:** 145–154

Collings DA, Harper JDI, Vaughn KC (2003) The association of peroxisomes with the developing cell plate in dividing onion root cells depends on actin microfilaments and myosin. Planta **218:** 204–216

Considine MJ, Wan YZ, D'Antuono MF, Zhou Q, Han MY, Gao H, Wang M (2012) Molecular genetic features of polyploidization and aneuploidization reveal unique patterns for genome duplication in diploid Malus. PLoS ONE **7:** e29449

Consiglio F, Carputo D, Monti L, Conicella C (2004) Exploitation of genes affecting meiotic non-reduction and nuclear restitution: Arabidopsis as a model? Sex Plant Reprod **17:** 97–105

Cui LY, Wall PK, Leebens-Mack JH, Lindsay BG, Soltis DE, Doyle JJ, Soltis PS, Carlson JE, Arumuganathan K, Barakat A, et al (2006) Widespread genome duplications throughout the history of flowering plants. Genome Res **16:** 738–749

Danilchik MV, Funk WC, Brown EE, Larkin K (1998) Requirement for microtubules in new membrane formation during cytokinesis of Xenopus embryos. Dev Biol **194:** 47–60

d'Erfurth I, Cromer L, Jolivet S, Girard C, Horlow C, Sun YJ, To JPC, Berchowitz LE, Copenhaver GP, Mercier R (2010) The cyclin-A CYCA1; 2/TAM is required for the meiosis I to meiosis II transition and cooperates with OSD1 for the prophase to first meiotic division transition. PLoS Genet **6:** e1000989

d'Erfurth I, Jolivet S, Froger N, Catrice O, Novatchkova M, Mercier R (2009) Turning meiosis into mitosis. PLoS Biol **7:** e1000124

d'Erfurth I, Jolivet S, Froger N, Catrice O, Novatchkova M, Simon M, Jenczewski E, Mercier R (2008) Mutations in AtPS1 (Arabidopsis thaliana parallel spindle 1) lead to the production of diploid pollen grains. PLoS Genet **4:** e1000274

De Storme N, Geelen D (2011) The Arabidopsis mutant *jason* produces unreduced first division restitution male gametes through a parallel/fused spindle mechanism in meiosis II. Plant Physiol **155:** 1403–1415

Dirks R, van Dun K, de Snoo CB, van den Berg M, Lelivelt CLC, Voermans W, Woudenberg L, de Wit JPC, Reinink K, Schut JW, et al (2009) Reverse breeding: a novel breeding approach based on engineered meiosis. Plant Biotechnol J **7:** 837–845

Dufresne F, Hebert PDN (1998) Temperature-related differences in life-history characteristics between diploid and polyploid clones of the Daphnia pulex complex. Ecoscience **5:** 433–437

Durbarry A, Vizir I, Twell D (2005) Male germ line development in Arabidopsis: *duo pollen* mutants reveal gametophytic regulators of generative cell cycle progression. Plant Physiol **137:** 297–307

Endlé MC, Stoppin V, Lambert AM, Schmit AC (1998) The growing cell plate of higher plants is a site of both actin assembly and vinculin-like antigen recruitment. Eur J Cell Biol **77:** 10–18

Flovik K (1940) Chromosome numbers and polyploidy within the flora of Spitzbergen. Hereditas **26:** 430–440

Francis KE, Lam SY, Copenhaver GP (2006) Separation of Arabidopsis pollen tetrads is regulated by *QUARTET1*, a pectin methylesterase gene. Plant Physiol **142:** 1004–1013

Francis KE, Lam SY, Harrison BD, Bey AL, Berchowitz LE, Copenhaver GP (2007) Pollen tetrad-based visual assay for meiotic recombination in Arabidopsis. Proc Natl Acad Sci USA **104:** 3913–3918

Grelon M, Vezon D, Gendrot G, Pelletier G (2001) AtSPO11-1 is necessary for efficient meiotic recombination in plants. EMBO J **20:** 589–600

Guggisberg A, Mansion G, Kelso S, Conti E (2006) Evolution of biogeographic patterns, ploidy levels, and breeding systems in a diploid-polyploid species complex of Primula. New Phytol **171:** 617–632

Gupta ML Jr, Bode CJ, Dougherty CA, Marquez RT, Himes RH (2001) Mutagenesis of beta-tubulin cysteine residues in Saccharomyces cerevisiae: mutation of cysteine 354 results in cold-stable microtubules. Cell Motil Cytoskeleton **49:** 67–77

Hermsen JGT (1984) Mechanisms and genetic implications of 2n gamete formation. Iowa State J Res **58:** 421–434

Higaki T, Kutsuna N, Sano T, Hasezawa S (2008) Quantitative analysis of changes in actin microfilament contribution to cell plate development in plant cytokinesis. BMC Plant Biol **8:** 80

Hulskamp M, Parekh NS, Grini P, Schneitz K, Zimmermann I, Lolle SJ, Pruitt RE (1997) The STUD gene is required for male-specific cytokinesis after telophase II of meiosis in Arabidopsis thaliana. Dev Biol **187:** 114–124

Jiang H, Wang FF, Wu YT, Zhou X, Huang XY, Zhu J, Gao JF, Dong RB, Cao KM, Yang ZN (2009) MULTIPOLAR SPINDLE 1 (MPS1), a novel coiled-coil protein of Arabidopsis thaliana, is required for meiotic spindle organization. Plant J **59:** 1001–1010

Johnson-Brousseau SA, McCormick S (2004) A compendium of methods useful for characterizing Arabidopsis pollen mutants and gametophytically-expressed genes. Plant J **39:** 761–775

Jürgens G (2005) Cytokinesis in higher plants. Annu Rev Plant Biol **56:** 281–299

Köhler C, Mittelsten Scheid O, Erilova A (2010) The impact of the triploid block on the origin and evolution of polyploid plants. Trends Genet **26:** 142–148

Leitch AR, Leitch IJ (2008) Genomic plasticity and the diversity of polyploid plants. Science **320:** 481–483

Li YH, Shen YA, Cai C, Zhong CC, Zhu L, Yuan M, Ren HY (2010) The type II *Arabidopsis* formin14 interacts with microtubules and microfilaments to regulate cell division. Plant Cell **22:** 2710–2726

Li Z, Larson-Rabin Z, Masson PH, Day CD (2009) FZR2/CCS52A1 mediated endoreduplication in Arabidopsis development. Plant Signal Behav **4:** 451–453

Liu RH, Sun QY, Li YH, Jiao LH, Wang WH (2003) Effects of cooling on meiotic spindle structure and chromosome alignment within in vitro matured porcine oocytes. Mol Reprod Dev **65:** 212–218

Liu Z, Makaroff CA (2006) *Arabidopsis* separase AESP is essential for embryo development and the release of cohesin during meiosis. Plant Cell **18:** 1213–1225

Mable BK, Alexandrou MA, Taylor MI (2011) Genome duplication in amphibians and fish: an extended synthesis. J Zool **284:** 151–182

Magistrini M, Szöllösi D (1980) Effects of cold and of isopropyl-N-phenylcarbamate on the second meiotic spindle of mouse oocytes. Eur J Cell Biol **22:** 699–707

Magnard JL, Yang M, Chen YCS, Leary M, McCormick S (2001) The Arabidopsis gene *tardy asynchronous meiosis* is required for the normal pace and synchrony of cell division during male meiosis. Plant Physiol **127:** 1157–1166

Mason AS, Nelson MN, Yan GJ, Cowling WA (2011) Production of viable male unreduced gametes in Brassica interspecific hybrids is genotype specific and stimulated by cold temperatures. BMC Plant Biol **11:** 103

McHale NA (1983) Environmental induction of high-frequency 2n pollen formation in diploid Solanum. Can J Genet Cytol **25:** 609–615

Mercier R, Vezon D, Bullier E, Motamayor JC, Sellier A, Lefèvre F, Pelletier G, Horlow C (2001) SWITCH1 (SWI1): a novel protein required for the establishment of sister chromatid cohesion and for bivalent formation at meiosis. Genes Dev **15:** 1859–1871

Mok DWS, Peloquin SJ (1975) Three mechanisms of 2n pollen formation in diploid potatoes. Can J Genet Cytol **17:** 217–225

Negri V, Lemmi G (1998) Effect of selection and temperature stress on the production of 2n gametes in Lotus tenuis. Plant Breed **117:** 345–349

Okamura S, Kakiuchi M, Sano A, Kawajiri M (1993) Loss of tubulin during cold treatment of cultured carrot cells. Physiol Plant **88:** 93–98

Orvar BL, Sangwan V, Omann F, Dhindsa RS (2000) Early steps in cold sensing by plant cells: the role of actin cytoskeleton and membrane fluidity. Plant J **23:** 785–794

Otegui MS, Staehelin LA (2004) Electron tomographic analysis of post-meiotic cytokinesis during pollen development in Arabidopsis thaliana. Planta **218:** 501–515

Pawlowski WP, Wang CJR, Golubovskaya IN, Szymaniak JM, Shi L, Hamant O, Zhu T, Harper L, Sheridan WF, Cande WZ (2009) Maize AMEIOTIC1 is essential for multiple early meiotic processes and likely required for the initiation of meiosis. Proc Natl Acad Sci USA **106:** 3603–3608

Pécrix Y, Rallo G, Folzer H, Cigna M, Gudin S, Le Bris M (2011) Polyploidization mechanisms: temperature environment can induce diploid gamete formation in Rosa sp. J Exp Bot **62:** 3587–3597

Peirson BN, Bowling SE, Makaroff CA (1997) A defect in synapsis causes male sterility in a T-DNA-tagged Arabidopsis thaliana mutant. Plant J **11:** 659–669

Peloquin SJ (1983) Genetic engineering with meiotic mutants. *In* DL Mulcahy, E Ottaviano, eds, Pollen: Biology and Implications for Plant Breeding. Elsevier Science, Amsterdam, pp 311–316

Peloquin SJ, Boiteux LS, Simon PW, Jansky SH (2008) A chromosome-specific estimate of transmission of heterozygosity by 2n gametes in potato. J Hered **99:** 177–181

Petrásek J, Schwarzerová K (2009) Actin and microtubule cytoskeleton interactions. Curr Opin Plant Biol **12:** 728–734

Pickering SJ, Braude PR, Johnson MH, Cant A, Currie J (1990) Transient cooling to room temperature can cause irreversible disruption of the meiotic spindle in the human oocyte. Fertil Steril **54:** 102–108

Preuss D, Rhee SY, Davis RW (1994) Tetrad analysis possible in Arabidopsis with mutation of the QUARTET (QRT) genes. Science **264:** 1458–1460

Quan L, Xiao R, Li W, Oh SA, Kong H, Ambrose JC, Malcos JL, Cyr R, Twell D, Ma H (2008) Functional divergence of the duplicated At-KIN14a and AtKIN14b genes: critical roles in Arabidopsis meiosis and gametophyte development. Plant J **53:** 1013–1026

Ramanna MS, Jacobsen E (2003) Relevance of sexual polyploidization for crop improvement: a review. Euphytica **133:** 3–18

Ramsey J (2007) Unreduced gametes and neopolyploids in natural populations of Achillea borealis (Asteraceae). Heredity (Edinb) **98:** 143–150

Ramsey J, Schemske DW (1998) Pathways, mechanisms, and rates of polyploid formation in flowering plants. Annu Rev Ecol Syst **29:** 467–501

Ravi M, Marimuthu MPA, Siddiqi I (2008) Gamete formation without meiosis in Arabidopsis. Nature **451:** 1121–1124

Rymen B, Fiorani F, Kartal F, Vandepoele K, Inzé D, Beemster GTS (2007) Cold nights impair leaf growth and cell cycle progression in maize through transcriptional changes of cell cycle genes. Plant Physiol **143:** 1429–1438

Sano T, Higaki T, Oda Y, Hayashi T, Hasezawa S (2005) Appearance of actin microfilament 'twin peaks' in mitosis and their function in cell plate formation, as visualized in tobacco BY-2 cells expressing GFP-fimbrin. Plant J **44:** 595–605

Singh M, Goel S, Meeley RB, Dantec C, Parrinello H, Michaud C, Leblanc O, Grimanelli D (2011) Production of viable gametes without meiosis in maize deficient for an ARGONAUTE protein. Plant Cell **23:** 443–458

Smertenko A, Draber P, Viklicky V, Opatrny Z (1997) Heat stress affects the organization of microtubules and cell division in Nicotiana tabacum cells. Plant Cell Environ **20:** 1534–1542

Soyano T, Nishihama R, Morikiyo K, Ishikawa M, Machida Y (2003) NQK1/NtMEK1 is a MAPKK that acts in the NPK1 MAPKKK-mediated MAPK cascade and is required for plant cytokinesis. Genes Dev **17:** 1055–1067

Spielman M, Preuss D, Li FL, Browne WE, Scott RJ, Dickinson HG (1997) TETRASPORE is required for male meiotic cytokinesis in Arabidopsis thaliana. Development **124:** 2645–2657

Stebbins GL (1984) Polyploidy and the distribution of the Arctic-Alpine flora: new evidence and a new approach. Bot Helv **94:** 1–13

Suzuki H, Kumai T, Matsuzaki M (2007) Effect of temperature decline on the cytoskeletal organization of the porcine oocyte. Journal of Mammalian Ova Research **24:** 107–113

Takahashi Y, Soyano T, Kosetsu K, Sasabe M, Machida Y (2010) HINKEL kinesin, ANP MAPKKKs and MKK6/ANQ MAPKK, which phosphorylates and activates MPK4 MAPK, constitute a pathway that is required for cytokinesis in Arabidopsis thaliana. Plant Cell Physiol **51:** 1766–1776

Talbert PB, Masuelli R, Tyagi AP, Comai L, Henikoff S (2002) Centromeric localization and adaptive evolution of an *Arabidopsis* histone H3 variant. Plant Cell **14:** 1053–1066

Tang ZH, Zhang LP, Yang D, Zhao CP, Zheng YL (2011) Cold stress contributes to aberrant cytokinesis during male meiosis I in a wheat thermosensitive genic male sterile line. Plant Cell Environ **34:** 389–405

Teige M, Scheikl E, Eulgem T, Dóczi R, Ichimura K, Shinozaki K, Dangl JL, Hirt H (2004) The MKK2 pathway mediates cold and salt stress signaling in Arabidopsis. Mol Cell **15:** 141–152

Twell D, Yamaguchi J, McCormick S (1990) Pollen-specific gene expression in transgenic plants: coordinate regulation of two different tomato gene promoters during microsporogenesis. Development **109:** 705–713

Valster AH, Pierson ES, Valenta R, Hepler PK, Emons AMC (1997) Probing the plant actin cytoskeleton during cytokinesis and interphase by profilin microinjection. Plant Cell **9:** 1815–1824

Van de Peer Y, Maere S, Meyer A (2009) The evolutionary significance of ancient genome duplications. Nat Rev Genet **10:** 725–732

Van der Elst J, Van den Abbeel E, Jacobs R, Wisse E, Van Steirteghem A (1988) Effect of 1,2-propanediol and dimethylsulphoxide on the meiotic spindle of the mouse oocyte. Hum Reprod **3:** 960–967

Wang WH, Meng L, Hackett RJ, Odenbourg R, Keefe DL (2001) Limited recovery of meiotic spindles in living human oocytes after cooling-rewarming observed using polarized light microscopy. Hum Reprod **16:** 2374–2378

Wang YX, Jha AK, Chen RJ, Doonan JH, Yang M (2010) Polyploidy-associated genomic instability in *Arabidopsis thaliana*. Genesis **48:** 254–263

Wang YX, Magnard JL, McCormick S, Yang M (2004) Progression through meiosis I and meiosis II in Arabidopsis anthers is regulated by an A-type cyclin predominately expressed in prophase I. Plant Physiol **136:** 4127–4135

Watanabe K, Peloquin SJ, Endo M (1991) Genetic significance of mode of polyploidization: somatic doubling or 2n gametes. Genome **34:** 28–34

Wijnker E, van Dun K, de Snoo CB, Lelivelt CLC, Keurentjes JJB, Naharudin NS, Ravi M, Chan SWL, de Jong H, Dirks R (2012) Reverse breeding in Arabidopsis thaliana generates homozygous parental lines from a heterozygous plant. Nat Genet **44:** 467–470

Wood TE, Takebayashi N, Barker MS, Mayrose I, Greenspoon PB, Rieseberg LH (2009) The frequency of polyploid speciation in vascular plants. Proc Natl Acad Sci USA **106:** 13875–13879

Wu S, Scheible WR, Schindelasch D, Van Den Daele H, De Veylder L, Baskin TI (2010) A conditional mutation in Arabidopsis thaliana separase induces chromosome non-disjunction, aberrant morphogenesis and cyclin B1;1 stability. Development **137:** 953–961

Xu C, Liu Z, Zhang L, Zhao C, Yuan S, Zhang F (2012) Organization of actin cytoskeleton during meiosis I in a wheat thermo-sensitive genic male sterile line. Protoplasma (in press)

Yamauchi A, Hosokawa A, Nagata H, Shimoda M (2004) Triploid bridge and role of parthenogenesis in the evolution of autopolyploidy. Am Nat **164:** 101–112

Yang XH, Boateng KA, Strittmatter L, Burgess R, Makaroff CA (2009) Arabidopsis separase functions beyond the removal of sister chromatid cohesion during meiosis. Plant Physiol **151:** 323–333

Yang XH, Boateng KA, Yuan L, Wu S, Baskin TI, Makaroff CA (2011) The radially swollen 4 separase mutation of Arabidopsis thaliana blocks chromosome disjunction and disrupts the radial microtubule system in meiocytes. PLoS ONE **6:** e19459

Zeng QN, Chen JG, Ellis BE (2011) AtMPK4 is required for male-specific meiotic cytokinesis in Arabidopsis. Plant J **67:** 895–906